AD_____

Grant Number DAMD17-96-1-6181

TITLE: Role of Bcl-2 in Breast Cancer Progression

PRINCIPAL INVESTIGATOR: Hyeong-Reh Kim, Ph.D.

CONTRACTING ORGANIZATION: Wayne State University
Detroit, Michigan 48202

REPORT DATE: September 1997

TYPE OF REPORT: Annual

PREPARED FOR: U.S. Army Medical Research and Materiel Command
Fort Detrick, Maryland 21702-5012

DISTRIBUTION STATEMENT: Approved for public release;
distribution unlimited

REPORT DOCUMENTATION PAGE

Form Approved
OMB No. 0704-0188

1. AGENCY USE ONLY *(Leave blank)*

2. REPORT DATE
September 1997

3. REPORT TYPE AND DATES COVERED
Annual (1 Aug 96 - 31 Jul 97)

4. TITLE AND SUBTITLE
Role of Bcl-2 in Breast Cancer Progression

5. FUNDING NUMBERS
DAMD17-96-1-6181

6. AUTHOR(S)
Hyeong-Reh Kim, Ph.D.

7. PERFORMING ORGANIZATION NAME(S) AND ADDRESS(ES)
Wayne State University
Detroit, Michigan 48202

8. PERFORMING ORGANIZATION REPORT NUMBER

9. SPONSORING/MONITORING AGENCY NAME(S) AND ADDRESS(ES)
U.S. Army Medical Research and Materiel Command
Fort Detrick, Maryland 21702-5012

10. SPONSORING/MONITORING AGENCY REPORT NUMBER

11. SUPPLEMENTARY NOTES

12a. DISTRIBUTION / AVAILABILITY STATEMENT
Approved for public release; distribution unlimited

12b. DISTRIBUTION CODE

13. ABSTRACT *(Maximum 200*

The anti-apoptotic gene bcl-2 is frequently overexpressed in many human tumors including invasive breast cancer. *In vitro* studies clearly demonstrate that the bcl-2 gene product prevents apoptosis following a variety of stimuli including radiation, hyperthermia, growth factor withdrawal and chemotherapeutic drugs. However, high levels of the bcl-2 expression have shown a positive correlation in clinicopathological studies, such as tumor grade and better response to hormonal treatment and chemotherapy. It is now critical to investigate the *in vivo* function of bcl-2 in human cells to elucidate the contradiction between clinical studies and *in vitro* studies. We have investigated the roles of bcl-2 in breast cancer development using MCF10A *in vitro* model and MCF10AT *in vivo* model. Here, we report that bcl-2 deregulates a G_1/S checkpoint in MCF10A cells through upregulation of G_1 cyclin activities, suggesting a role of bcl-2 as an oncogene. We then show that bcl-2 induces transformed phenotype in MCF10AT cells as determined by a soft agar assay. Bcl-2 expressing MCF10AT cells will be utilized for in vivo studies.

14. SUBJECT TERMS
Breast Cancer, Apoptosis, Cell Cycle, Progression

15. NUMBER OF PAGES
54

16. PRICE CODE

17. SECURITY CLASSIFICATION OF REPORT	18. SECURITY CLASSIFICATION OF THIS PAGE	19. SECURITY CLASSIFICATION OF ABSTRACT	20. LIMITATION OF ABSTRACT
Unclassified	Unclassified	Unclassified	Unlimited

FOREWORD

Opinions, interpretations, conclusions and recommendations are those of the author and are not necessarily endorsed by the U.S. Army.

____ Where copyrighted material is quoted, permission has been obtained to use such material.

____ Where material from documents designated for limited distribution is quoted, permission has been obtained to use the material.

✓ Citations of commercial organizations and trade names in this report do not constitute an official Department of Army endorsement or approval of the products or services of these organizations.

✓ In conducting research using animals, the investigator(s) adhered to the "Guide for the Care and Use of Laboratory Animals," prepared by the Committee on Care and Use of Laboratory Animals of the Institute of Laboratory Resources, National Research Council (NIH Publication No. 86-23, Revised 1985).

____ For the protection of human subjects, the investigator(s) adhered to policies of applicable Federal Law 45 CFR 46.

✓ In conducting research utilizing recombinant DNA technology, the investigator(s) adhered to current guidelines promulgated by the National Institutes of Health.

✓ In the conduct of research utilizing recombinant DNA, the investigator(s) adhered to the NIH Guidelines for Research Involving Recombinant DNA Molecules.

✓ In the conduct of research involving hazardous organisms, the investigator(s) adhered to the CDC-NIH Guide for Biosafety in Microbiological and Biomedical Laboratories.

9-24-97

PI - Signature Date

TABLE OF CONTENTS

Introduction

The proto-oncogene bcl-2 was originally discovered by virtue of its translocation into the immunoglobulin locus in follicular B-cell lymphoma (1). Overexpression of bcl-2 under the immunoglobulin promoter induces follicular hyperplasia in transgenic mice, demonstrating the role of bcl-2 as an oncogene (2, 3). Bcl-2 is frequently overexpressed in many human tumors including invasive breast cancers (4,5). *In vitro* studies clearly demonstrate that the bcl-2 gene product prevents apoptosis following a variety of stimuli including radiation, hyperthermia, growth factor withdrawal and chemotherapeutic drugs. However, high levels of the bcl-2 expression has shown a positive correlation in clinicopathological studies, such as tumor grade and better response to hormonal treatment and chemothearpy (6). It is now critical to investigate the *in vivo* function of bcl-2 in human cells to elucidate the contradiction between clinical studies and *in vitro* studies. We have investigated the roles of bcl-2 in breast cancer development using MCF10A *in vitro* model and MCF10AT *in vivo* model.

MCF10A *in vitro* model to study development of human breast cancer.
Studies of the roles of specific genes to initiate transformation of breast epithelial cells have been hindered by scarcity of nonmalignant human mammary epithelial cell lines. In our institution, MCF10A cell line was established without viral or chemical intervention from immortal diploid human breast epithelial cells, to study sequential development of differentiated or malignant states of breast epithelial cells (7). Using MCF10A cells, we have found that bcl-2 deregulates cell cycle (ref. 8 and data shown below) and induces partially transformed phenotype as determined by foci formation assay (data not shown). MCF10A cells thus provide an *in vitro* model system to study interactions of oncogene-induced signal transduction pathways in normal breast epithelial cells leading to the transformed phenotype.

MCF10AT *in vivo* model to study human breast cancer progression
Preneoplasia and progression of mammary cancer have been defined almost exclusively by studies of mouse hyperplastic alveolar nodules (HANS). The HAN lesions in normal mice are morphologically similar to normal mammary tissue in pregnant mice but are hormone independent and carcinomas arise sporadically from a homogeneous field of morphologically normal, albeit preneoplastic, alveolar-ductule tissue. Although these mouse mammary models have been the basis for much information regarding the basic biology of mammary cancer, a number of differences in the histology and biology of mouse and human mammary lesions exist. Dr. Miller (consultant in this application) and his colleagues have developed an *in vivo* model system to study human breast cancer progression (9-11); Whereas MCF10A cells do not survive *in vivo* in immune deficient mice, c-Ha-ras oncogene transfected MCF10A cells (MCF10AneoT) form small nodules in Nude/Beige mice which persist for at least one year and sporadically progress to carcinomas. By establishing cells in tissue culture from one carcinoma, a cell line designated MCF10AT1 was derived which forms simple ducts when transplanted in Matrigel into immune deficient mice. With time *in vivo*, the epithelium becomes proliferative and a cribriform pattern develops within the xenografts. A significant number progress to lesions resembling atypical hyperplasia and carcinomas *in situ* in women and approximately 25% continue to progress to invasive carcinomas with various types of differentiation including glandular, squamous, and undifferentiated. Cells have been established in cultures from lesions representing 4 successive transplant generations. With each generation, cells are somewhat more likely to progress to high risk lesions resembling human proliferative breast disease. Although the incidence of invasive carcinoma remains fairly constant at 20-25%, the frequency of nodules showing proliferative breast disease rose from 23% in the first transplant generation to 56% in the fourth transplant generation (9-11) These cells, most probably subsequent to genetic alterations, are capable of reproducing the pathology of proliferative breast disease seen in women and ultimately progressing to neoplasia. Thus, the MCF10AT model provides a setting in which the steps in the conversion of the breast ductal epithelial cell to a malignant disease can be studied.

Body of Report

During the 1996-1997 period, we have focused on the role of bcl-2 on cell cycle regulation. We have also established bcl-2 overexpressing MCF10ATG3B cells (the third transplant generation of MCF10AT cells) to study in vivo function of bcl-2.

Methods

Northern blot analysis
MCF10A and bcl-2 overexpressing MCF10A clones (MCF10A bcl-2-2 and MCF10A bcl-2-30, see ref. 8 for establishment of bcl-2 overexpressing MCF10A cells) were cultured as previously described (7). Cells were growth-arrested by culturing in serum -free medium for 48 hours at confluency. Cells were then treated with regular MCF10A medium containing 5% horse serum to induce the cell cycle. At various times between 0-24 hr after serum-stimulation, total cellular RNA was isolated using the guanidium-thiocyanate method. Five μg of each sample were denatured and separated on a 1% formaldehyde-agarose gel. The levels of $p21^{WAF1/CIP1}$ mRNAs were determined as previously described (8).

Western blot analysis
MCF10A, MCF10A bcl-2-2 and MCF10A bcl-2-30 cells were serum starved as described above. Quiescent cells were treated with MCF10A medium to trigger the cell cycle. At various times between 0-24 hrs, whole-cell extracts were prepared as previously described (8). Protein concentrations were measured using bicinchoninic acid protein assay reagents (Pierce, Chicago, IL). Cell lysates (20 μg/lane)were denatured, subjected to SDS-PAGE analysis, and then electrophoretically transferred to nitrocellulose membrane. Membranes were incubated with anti-$p21^{WAF1/CIP1}$ antibody (Ab-1, Oncogene Science) or anti-pRb antibody (IF8, Santa Cruz Biotechnology). $p21^{WAF1/CIP1}$ and pRb proteins were visualized using HRP-conjugated goat anti-mouse IgG (1: 3000 dilution) and chemiluminescence reagent (Dupont, Boston MA 02118). The membranes were exposed to X ray film from 1 to 15 mins.

Kinase assay
Cells will be lysed in 50 mM Tris (pH 8.0), 120 mM NaCl, 50 mM NaF, 0.1 mM sodium vanadate, 2 mM EDTA, 10 μg/ml each of chymostatin, leupeptin, antipain, and pepstatin A, 2 μg/ml 4-(2-aminoethyl)benzenesulfonyl fluoride (Calbiochem), and 0.4 % Nonidet P-40. The extracts will be clarified by centrifugation at 14,000 rpm for 15 min at 4 ^{0}C. For each condition, triplicate plates will be lysed and assayed independently. Lysates will be incubated for 1.5 h at 4 ^{0}C with monoclonal antibody against cyclin E or cyclin D (purchased from Santa Cruz Biotechnology). Immune complexes will be collected using 20 μl of protein G-Sepharose and washed 3 times with 1.0 ml of lysis buffer and once with 1 ml of 20 mM Tris (pH 7.5)-10 mM $MgCl_2$. Kinase assays will be performed in 65 mM K-β-glycerophosphate (pH 7.3), 15 mM $MgCl_2$, 16 mM EGTA, 10 mM DTT, 1 mg/ml ovalbumin, 0.5 mM NaF, 0.1 mM sodium orthovandate, 5 μg/ml leupeptin, and [γ-^{32}P]ATP (0.01-0.3 nCi/pmol) using 0.1 ml (one-tenth of the immune complex) and substrates (2.5 μM histone H1 for cyclin E assay or Rb protein for cyclin D assay). After 15 min at 37 ^{0}C, 10 μl aliquots will be removed and spotted on phosphocellulose paper for quantitation, and the remainder will be mixed with 2x SDS buffer prior to SDS-PAGE, autoradiography, and quantitated by scanning.

^{3}H-thymidine incorporation assay
MCF10A, MCF 10A bcl-2-2 or MCF 10A bcl-2-30 cells were plated in 24-well plates ($2x10^4$ cells per well) using regular MCF10A medium containing 5% horse serum . To induce cell-cycle arrest, cells were washed with phosphate-buffered saline and cultured in serum-free medium for 48 hours. Cells were then treated with regular MCF10A medium containing 5% horse serum and ^{3}H-thymidine (0.25 μCi). At various times between 0 and 48 hr, cells were washed with cold

PBS, followed by 10% TCA and methanol. One-half ml of 0.5 N NaOH was added to each well and the cell lysates were collected in scintillation vials for counting radioactivity. All experiments were done in triplicate.

Determination of cell cycle distribution

Percentage of cells in each cell cycle phase was determined by flow cytometry (PAS-II, Partec AG, Germany). Confluent cells were washed with PBS and cultured in serum-free media for 48 hours. To induce cell cycle, cells were trypsinized, plated at $2x10^6$ cells/100 mm plate and cultured in regular MCF10A medium for various times between 0-48 hr. Cells were trypsinized, suspended in regular MCF10A medium, centrifuged at 150 *g* for 5 min and fixed with 70% ethanol. The fixed cells were spun down and the cell pellet was resuspended in Hoechst staining solution at a concentration of 1 $x10^6$ cells/ml and incubated for 3 min at room temperature. The staining solution consisted of 3 μg/ml Hoechst 33258 (Sigma Chemical Co., St. Louis, MO) in Tris buffer (2 mM $MgCl_2$, 0.1% Triton X-100, 154 mM NaCl, 100 mM Tris, pH 7.5). The stained cells (30,000) were analyzed by flow cytometry. Optical filtration included a UG-1 excitation filter, a 420 nm dichroic filter and 435 nm long pass emission filter. Single-channel data were acquired and subsequently analyzed with a computer program (Phoenix Flow Systems,).

Assay for growth in soft agar

Soft agar assays were performed in six-well plates using a 1-ml base layer of 0.6% agar in MCF10A medium. A total of 5000 cells in 0.3% top agar were plated in each well. Fresh top agar was overlaid every 5 days. After 2 weeks, positive colonies (>0.1 mm diameter) were scored as previously described (12)

Results

We previously reported that bcl-2 downregulates basal level expression and radiation-induced expression of $p21^{WAF1/CIP1}$ in MCF10A cells (8). Since $p21^{WAF1/CIP1}$ is an inhibitor of cyclin dependent kinase and play an important role in G1/S checkpoint, we have investigated the impact of bcl-2 overexpression on the levels of $p21^{WAF1/CIP1}$ expression during the serum-induced cell cycle. Control and bcl-2 overexpressing MCF10A cells were synchronized at G_0 as described in Materials and Methods. The levels of $p21^{WAF1/CIP1}$ transcripts during the serum-induced cell cycle are shown in **Fig. 1A and B**. When quiescent control MCF10A cells entered the cell cyclè upon serum treatment, $p21^{WAF1/CIP1}$ mRNA was rapidly induced and maintained at an elevated level for more than 6 hours. $p21^{WAF1/CIP1}$ transcript levels in bcl-2 transfected MCF10A clones were induced upon serum treatment at a much lesser extent and decreased toward basal levels at about 3 h (note that RNA at 0 hr in MCF10A bcl-2-2 clone was overloaded as shown in lane 7 in Fig. 1B). The levels of bcl-2 protein did not change during the cell cycle and the bcl-2 protein levels were consistently higher in bcl-2 transfected cells as shown in **Fig. 1C and D** . The levels of $p21^{WAF1/CIP1}$ protein were significantly downregulated by bcl-2 overexpression during the early time points corresponding to G_0 and G_1 as shown in Fig 4 and 5. This result suggests that the basal level of $p21^{WAF1/CIP1}$ expression is downregulated by bcl-2, whereas serum-induced $p21^{WAF1/CIP1}$ expression is less affected by bcl-2 overexpression.

To determine the effect of bcl-2 downregulation of $p21^{WAF1/CIP1}$ on kinase activity of the cyclin-dependent kinase (cdk) complex during the cell cycle, we examined the status of phosphorylation of pRb, one of the major target genes of cdks. The time course of appearance of phosphorylated pRb following serum stimulation in control and bcl-2 overexpressing MCF10A cells is shown in **Fig. 2**. The hyperphosphorylated form of pRb (upper arrowhead) is distinguished from the underphosphorylated form of pRb (lower arrowhead) by SDS-PAGE due to differences in the migration rates. As shown in Fig 2A, the phosphorylated form of pRb was barely detectable after 9 hr of serum treatment in control MCF10A cells. In contrast,

phosphorylated pRb was detected early in bcl-2 overexpressing MCF10A cells. Clone 30 contained phosphorylated pRb after 7 hr of serum treatment and clone 2 after 5 hr. These studies suggest that $p21^{WAF1/CIP1}$ downregulation by bcl-2 overexpression at early time points during serum-induced cell cycle results in early activation of cdks which phosphorylate their target gene products, including pRb. We have measured activities of G1 cyclins (cyclin D_1, D_2, D_3 and Cyclin E) *in vitro*. As shown in **Fig. 3**, Cyclin D1 dependent kinase is activated 1.5 hr after serum stimulation and maintained at high level more than 9 hours in bcl-2 overexpressing cells, whereas its activity is transiently induced approximately 4 hr after serum stimulation in the control MCF10A cells. We are currently measuring cyclin D_2, D_3 or Cyclin E dependent kinase activities in vitro.

Since cdks and their inhibitors are critical in controlling precisely the order and timing of cell cycle events, we next examined whether activation of cdks in bcl-2 overexpressing cells during serum-induced cell cycle affects G_1 duration. The cell cycle was induced by the addition of serum in the presence of ^{3}H-thymidine. The onset of DNA synthesis was determined by measuring incorporation of ^{3}H-thymidine into cells during the time period from 0 to 48 hours. As shown in **Fig.4**, ^{3}H-thymidine incorporation is higher in bcl-2 overexpressing cells than in the control cells. In addition, half maximal incorporation required 15 hours of serum treatment in bcl-2 overexpressing cells, whereas 18 hours were required in the control cells. These results suggest that bcl-2 overexpressing cells enter S phase faster and in larger numbers as compared to the control cells. To confirm this finding, we analyzed cell cycle distribution of the control and bcl-2 overexpressing MCF10A cells by flow cytometric analysis (**Fig. 5**). To induce cell cycle, quiescent cells were trypsinized and replated using MCF10A medium for various times between 0-48 hours. At 20 hr after stimulation, most of the neo-resistant marker transfected control cells remained in G1, whereas 23-38% of bcl-2 transfected cells entered S phase. Entry into the cell cycle was delayed when determined by flow cytometry as compared to the ^{3}H-thymidine incorporation assay. We attribute this difference to the fact that the cells were trypsinized to induce the cell cycle for flow cytometry, whereas the cells were stimulated with serum without trypsinization for the ^{3}H-thymidine incorporation assay. Although bcl-2 overexpressing cells enter S phase faster from quiescent phase, the rate of cell proliferation is not increased (data not shown).

Anti-oncogenic activities of p53 and pRb appear to be related to their abilities to control the cell cycle (13-20). Since our studies suggest that bcl-2 overexpression deregulates activities of these molecules, we wished to examine the effects of bcl-2 overexpression on transformation of breast epithelial cells. To develop in vivo model to study the roles of bcl-2, we have transfected bcl-2 into MCF10ATG3B cells (the third transplant generation of MCF10AT cells). Bcl-2 transfected MCF10AneoT cells were selected for hygromycin-resistant phenotype and levels of bcl-2 expression were determined by western blot analysis (**Fig. 6**). We then investigated whether bcl-2 enhances transformed phenotype of breast epithelial cells in MCF10ATG3B cells. To address this, we determined anchorage-independent growth in soft agar. As shown in **Fig. 7**, Bcl-2 expressing cells form colonies at an average efficiency of 20-22%, whereas control MCF10ATG3B cells have an average colony efficiency of less than 2%.

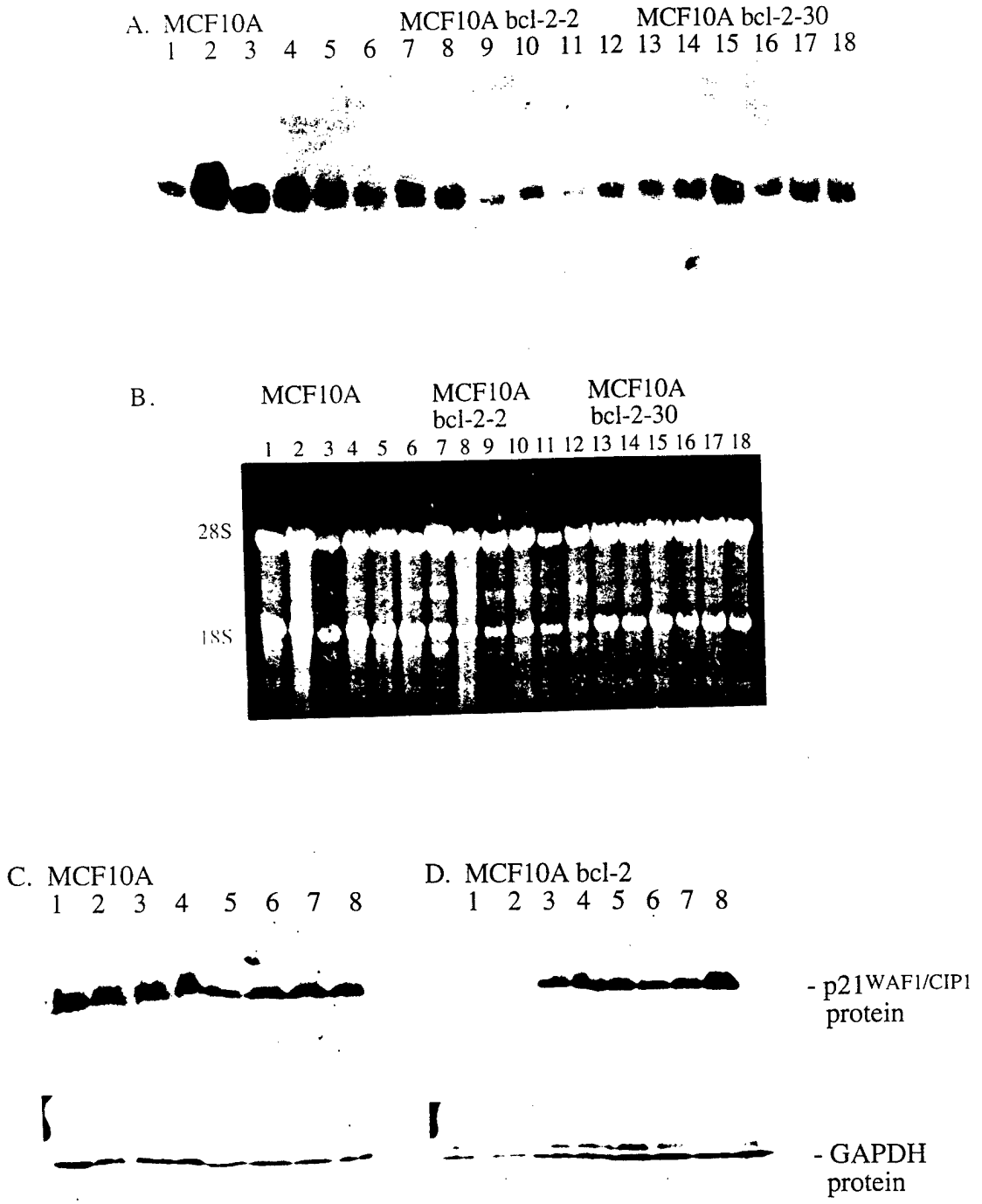

Fig. 1. Effects of bcl-2 overexpression on serum-induced p21WAF1/CIP1 expression during the cell cycle. A. Northern blot analysis of p21WAF1/CIP1. Confluent control MCF10A (lanes 1-6), bcl-2 overexpressing MCF10A clone 2 (lanes 7-12) and clone 30 (lanes 13-18) were cultured in serum free DMEM/F12 medium for 48 hours. At various time points after serum treatment [O hr (lanes 1,7 and 13); 30 min (lanes 2, 8 and 14); 3 hr (lanes 3, 9,

and 15); 6 hr (lanes 4, 10 and 16); 12 hr (lanes 5, 11 and 17); 24 hr (lanes 6, 12 and 18), total RNAs were extracted . The levels of p21WAF1/CIP1 RNA were detected using human p21WAF1/CIP1 cDNA probe. B. In order to confirm the amount and quality of RNAs loaded in each lane, RNAs were stained with ethidium bromide. Top panels in C and D. Western blot analysis of p21WAF1/CIP1. MCF10A (C) and bcl-2 overexpressing MCF10A clone 2 (D) were arrest at G_0 as described above. At various time points after serum treatment [0 hr (lanes 1); 5 hr (lanes 2); 7 hr (lanes 3); 9 hr (lanes 4); 12 hr (lanes 5); 15 hr (lanes 6); 18 hr (lanes 7); 24 hr (lanes 8)]. Bottom panels in C. and D. In order to confirm the amount of proteins loaded in each lane, the identical blots were probed with anti-glyceraldehyde 3-phosphate dehydrogenase (GAPDH) antibody (Biologicals).

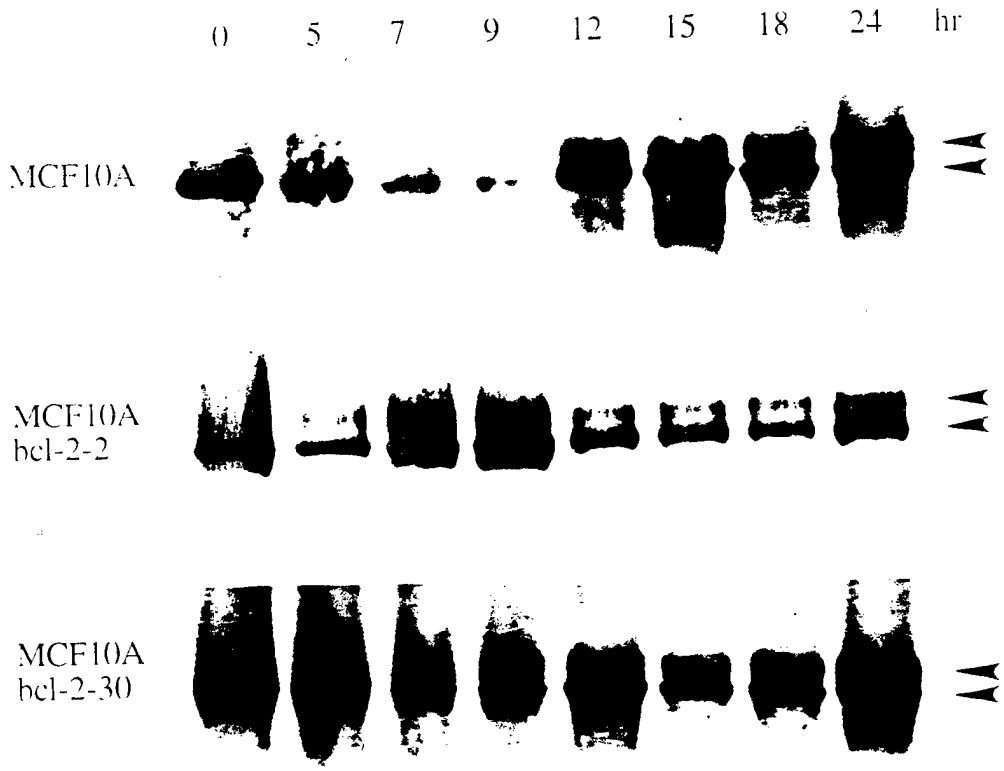

Fig. 2. Effects of bcl-2 overexpression on phosphorylation of pRb during the cell cycle. Confluent control MCF10A, bcl-2 overexpressing MCF10A clone 2 and clone 30 were cultured in serum free DMEM/F12 medium for 48 hours. At the indicated times after serum treatment, cells were lysed using SDS-sample buffer. Hyperphosphorylated form of pRb (slowly migrating form) and hypophosphorylated form of pRb (indicated as arrowheads)were detected using anti-pRb antibody (Oncogene Science) on a 6% polyacrylamide gel.

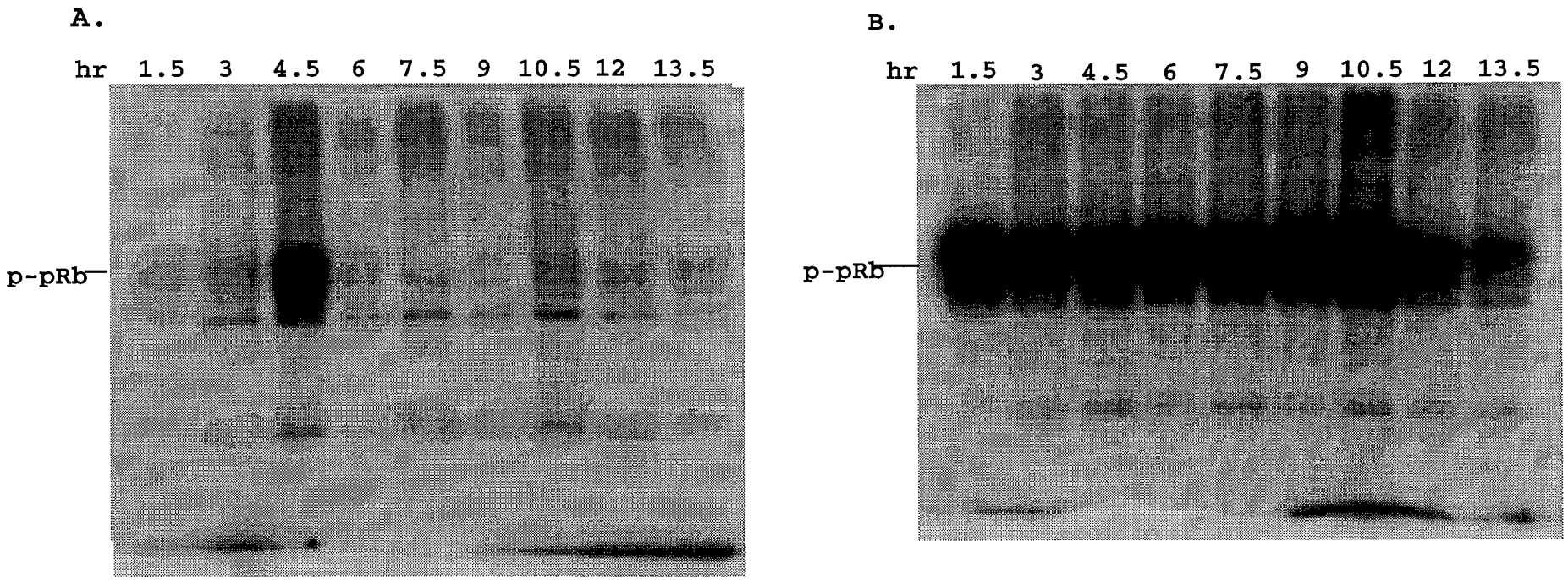

Fig. 3: **Analysis of cyclin D1-associated kinase activity in bcl-2 overexpressing human breast epithelial cells.**

Pooled populations of vector control (A) and bcl-2 overexpressing (B) MCF10A cells were synchronized at G_0 by serum deprivation for 48 hours. Cyclin D1 complexes were immunoprecipitated from extracts of cells stimulated with serum at different times. Kinase activity of the complexes was measured using purified GST-pRb fusion protein as the substrate.

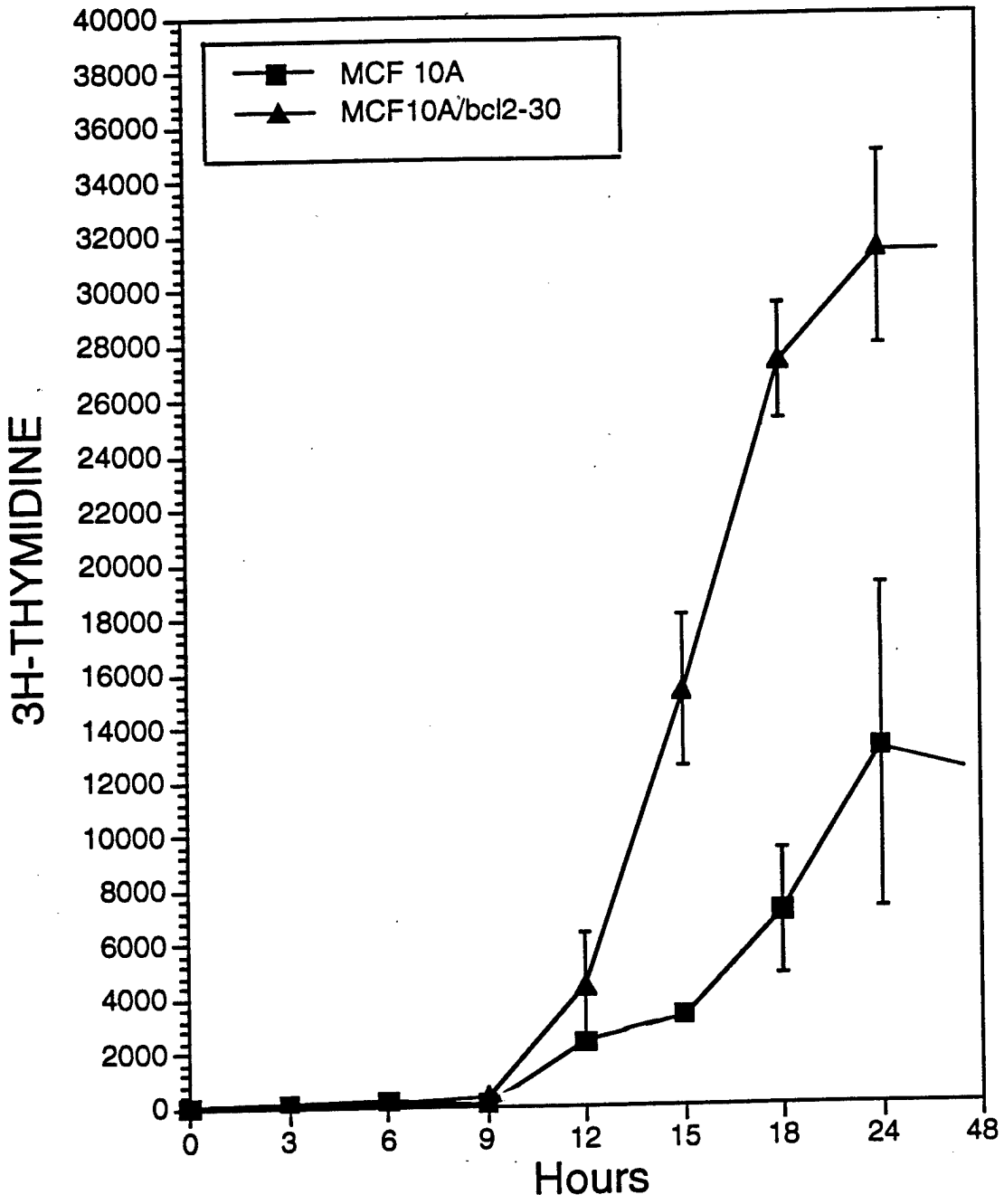

Fig. 4. ^{3}H-thymidine incorporation assay to determine the onset of DNA synthesis. Control MCF10A and bcl-2 overexpressing MCF10A clone 30 were cultured in serum free DMEM/F12 medium for 48 hours. At the indicated times after serum treatment in the presence of ^{3}H-thymidine, incorporation of 3H-thymidine into cells was measured during the time points from 0 to 48 hours. Experiments were performed in triplicate.

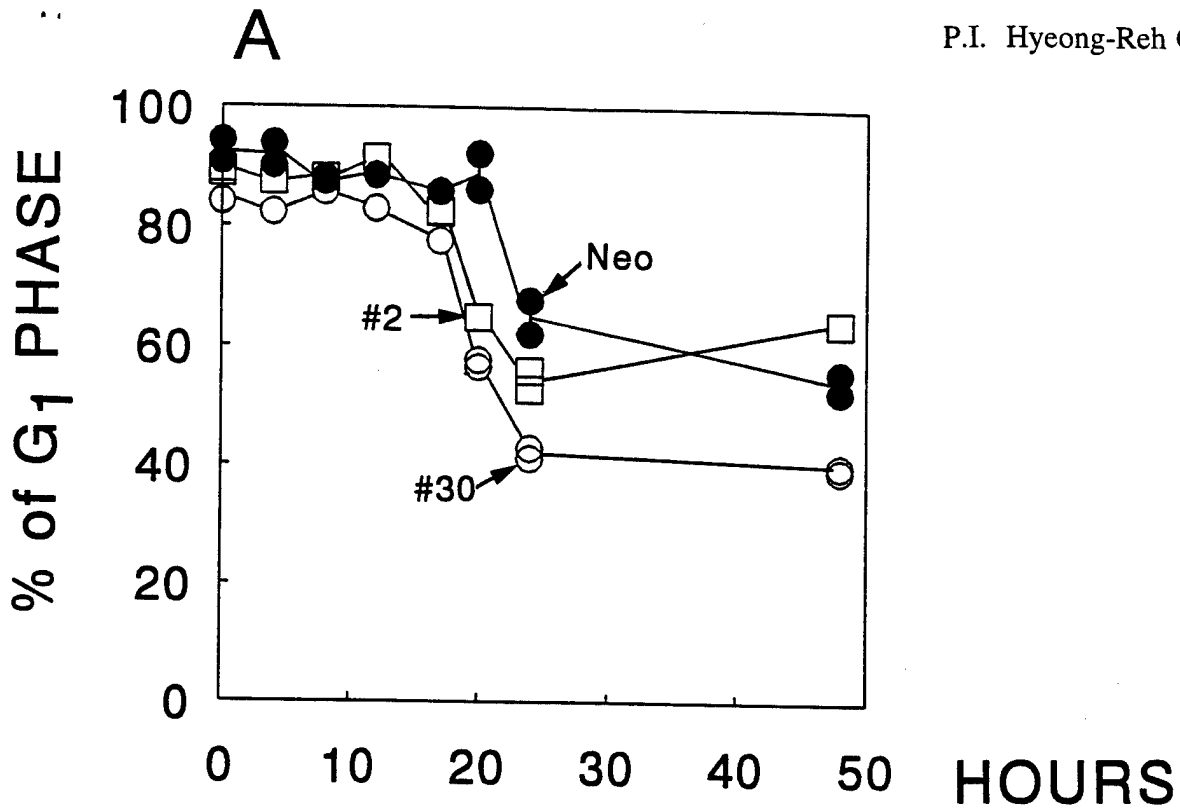

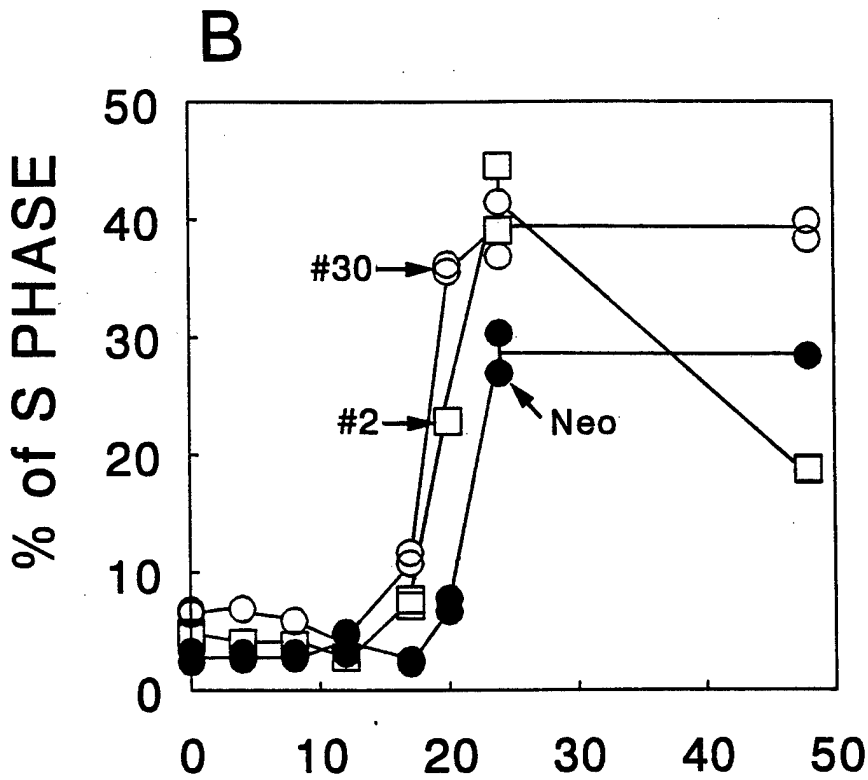

Fig.5. Cell cycle distributions during serum-stimulated cell proliferation. Percentages of cells in G_1 (A) or in S phase (B) were plotted against time after releasing from serum starvation. Neo, the neo-resistant marker transfected MCF10A cells; bcl-2-#2 and bcl-2-#30, bcl-2 overexpressing MCF10A clones

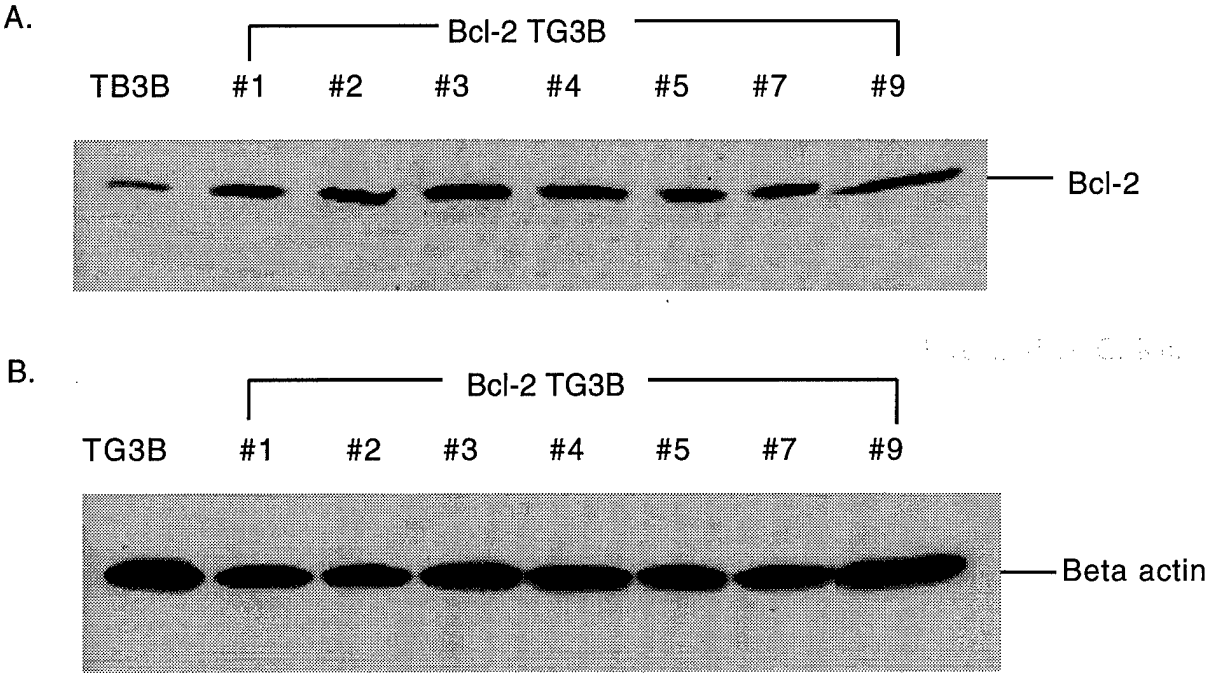

Fig. 6. Western blot analysis of the bcl-2 protein. The total protein from control (lane 1) and bcl-2 transfected MCF10ATG3B clones (lanes 2 to 8) were extracted. Levels of bcl-2 protein were determined using anti-bcl-2 Ab. To confirm the amount of protein loaded in each lane, the identical blot was probed anti-Beta actin Ab.

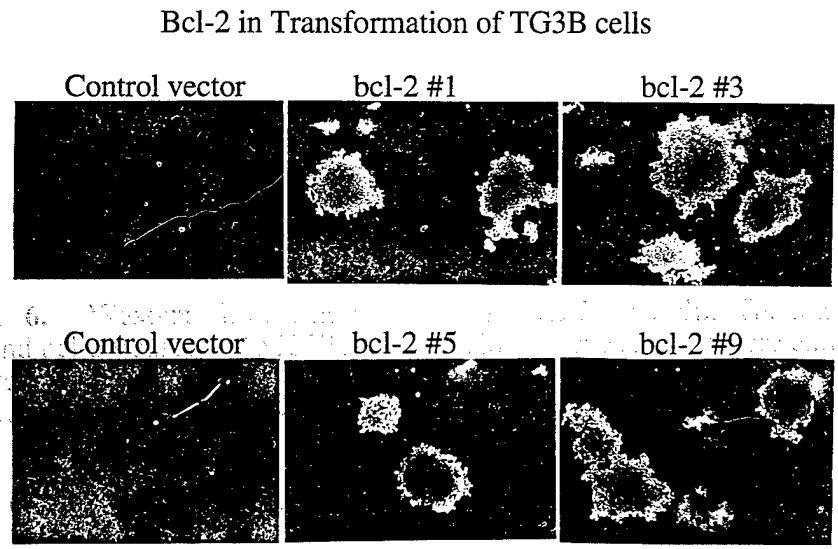

Fig. 7. Bcl-2 induces transformed phenotype in MCF10ATG3B cells. Control (hygromycin-resistant marker vector transfected) and bcl-2 overexpressing MCF 10ATG3B cells (clone 1, 3, 5, 9), were assayed for their abilities to grow in soft agar as a measurement of anchorage independent growth.

Conclusion

The roles of bcl-2 in the regulation of apoptosis and cell cycle regulation have been intensively studied using a variety of cell lines (largely hematopoietic cells). Mazel et al. (21) and Linette et al. (22) recently reported that increasing the levels of bcl-2 results in an increase in the length of G_1 phase in mouse T cells and isogenic FDC-P1 myelocytic cell lines. In these cells, bcl-2 upregulates the cdk inhibitor of $p27^{Kip1}$, but not $p21^{WAF1/CIP1}$(22), and results in a decrease in the ratio of hyperphosphorylated pRb /hypophosphorylated pRb (21). These findings lead to the hypothesis that bcl-2 inhibition of apoptosis is related to its ability to delay the cell cycle entry into S phase, which allows additional time for the cells to prepare for DNA synthesis and/or repair DNA damage (21).

In human breast epithelial cells, however, we found the opposite effect of bcl-2 on the cell cycle entry into S phase. Recently, bcl-2-mediated upregulation of G_1 cyclin activities and hyperphosphorylation of pRb were also reported in human prostate cancer cell (LNCaP) (23). These suggest that the effects of bcl-2 on cell cycle regulation may differ depending on cell types (e. g. hematopoietic cell *vs.* epithelial cell) and/or species . Involvement of bcl-2 in cancer development was believed to result from its ability to prevent cell death (thereby increase cell number). However, our results suggest that bcl-2 in breast epithelial cells may be involved in the transformation process, possibly through deregulation of cell cycle. Thus, it will be important to understand the biochemical and pathological effects of bcl-2 expression in human breast epithelial cells to understand human breast disease.

We will continue to investigate the roles of bcl-2 on cell cycle regulation and transformation of breast epithelial cells. As proposed in the original application, we will also investigate the bcl-2 effect on radiation induced transformation. In the next funding period, we would like to investigate the roles of bcl-2 in vivo using MCF10AT model (MCF10ATG3B cells).

References

1. Tsujimoto, Y., Cossman, J., Jaffe, E. and Croce, C. M. Involvement of the bcl-2 gene in human follicular lymphoma. Science (Washington DC), 228-1440-1143, 1985

2. McDonnell, T. J., Deane, N., Platt, F. M., Nunes, G., Jaeger, U., McKearn, J. P. and Korsmeyer, S. J. Bcl-2-immunoglobulin transgenic mice demonstrate extended B-cell survivlal and follicular lymphoproliferation. Cell 57, 79-88, 1989.

3. Strasser A., Harris, A. W and Cory, S. Bcl-2 transgene inhibits T-cell death and perturbs thymic self-censorship. Cell 67, 889-899, 1991.

4. Silvestrinii, R., Veneroni, S., Daidone, M. G., Benini, E., B., Boracchi, P., Mezzetti, M., Di Fronzo, G., Rilke, F., Veronesi, U. (1994) The Bcl-2 protein: a prognostic indicator strongly related to p53 protein in lymph node-negative breast cancer patients. J. Natl Cancer Inst. 86, 499-504

5. Siziopikou, K. P. , Prioleau, J. E. Harris, J. R. And Stuart J. S. Bcl-2 expression in the spectrum of preinvasive breast lesions. Cancer 77(3), 499-506, 1996

6. Visscher, D. W., Sarkar, F., Tabaczka, P., Crissman, J. Clinicopathologic analysis of bcl-2 immunostaining in breast carcinoma. Modern Pathology 9, 642-646, 1996

7. Soule H., Maloney, T. M., Wolman S. R., Peterspm, W. D., Brenz, R., McGrath, C. M., Russo, J., Pauley, R.J., Jones, R.F., and Brooks, S.C.(1990) .Isolation and characterization of a spontaneously immortalized human breast epithelial cell line, MCF-10. Can. Res. 50, 6075-6086

8. Upadhyay, S., Li, G., Liu, H., Chen, Y., Sarkar, F. And Kim, H.-R. C. Bcl-2 suppresses expression of p21WAF1/CIP1 in breast epithelial cells. Cancer Res. 55, 4520-4524, 1995

9. Miller, F. R., Soule, H. D., Tait, L., Pauley, R. J., Wolman, S. R., Dawson, P. J., Heppner, G. H. Xenograft model of progressive human proliferative breast disease. JNCI 85, 1725-1732, 1993

10. Dawson, P. J., Wolman, S. R., Tait, L., Heppner, G. H., Miller, F. R. MCF10AT: A model for the evolution of cancer from proliferative breast disease. Am. J. Path 148, 313-319, 1996

11. Miller, F. R. Models of progression spanning preneoplasia and metastasis: The human MCF10AneoT.TGn series and a panel of mouse mammary tumors. In: Mammary tumor cell cycle, differentiation and metastasis, ed. M.E. Lippman and R.B. Dickon, pp243-263. Kluwer Academic Publication, Boston, 1996

12. Kim, H.-R. C., Upadhyay, S., Korsmeyer, S. and Deuel, T. F. Platelet-derived growth factor (PDGF) B and A homodimers transform murine fibroblasts depending on the genetic background of the cell. J. Biol. Chem. 269, 30604-30608, 1994

13. Lin, D., Shields, M. T., Ullrich, S. J., Appella, E., and Mercer, W. E. Growth arrest induced by wild-type p53 protein blocks cells prior to or near the restirction point in late G_1 phase. Proc. Natl. Acad. Sci. USA 89(19), 9210-9214, 1992

14. Kastan, M. B., Onyekwere, O., Sidransky, D., Vogelstein, B., and Craig, R. W. Participation of p53 protein in the cellular response to DNA damage. Can. Res. 51, 6304-6311, 1991

15. Kuerbitz, S. J., Plunkett, B. S., Walsh, W. V., and Kastan, M. B. Wild-type p53 is a cell cycle checkpoint determinant following radiation. Proc. Natl. Acad. Sci. USA 89(16), 7491-7495, 1992

16. Kastan, M. B., Zhan, Q., el-Deiry, W., Carrier, F., Jacks, T., Walsh, W. V., Plunkett, B. S., Vogelstein, B., and Fornace, A. J. A mammalian cell cycle checkpoint pathway utilizing p53 and GADD45 is defective in ataxia-telangiectasia. Cell 71 (4), 587-597, 1992

17. Lane, D. P. Cancer. p53, guardian of the genome. Nature 358 (6381), 15-16, 1992

18. Lee, W.-H., SShew, J.-Y., Hong, F. D., Sery, T. W., Donoso, L. A., Young, L.-J., Bookstein, R., and Lee, E. Y-H.P. The retinoblastoma susceptibility gene encodes a nuclear phosphoprotein associated with DNA binding activity. Nature, 329, 642-645, 1987

19. Dowdy, S. F., Hinds, P. W., Louie, K., Reed, S. I., Arnold, A., and Weinberg, R. A. Physical interaction of the retinoblastoma protein with human D cyclins. Cell 73(3), 499-511, 1993

20. Nevins, J. R. E2F: A link between the Rb tumor suppressor protein and viral oncoproteins. Science 258, 424-429, 1992

21. Mazel S., Burtrum, D. and Petrie, H. Regulation of cell division cycle progression by bcl-2 expression : A potential mechanism for inhibition of programmed cell death. J. Exp. Med. 183, 2219-2226, 1996

22. Linette, G., Li, Y., Roth, K. And Korsmeyer, S. Cross talk between cell death and cell cycle

progression : Bcl-2 regulates NFAT-mediated activation. Proc. Natl. Acad. Sci. 93, 9545-9552, 1996

23. Day, M. L., Foster, R. G., Day, K. C., Zhao, X., Humphrey, P., Swanson, P., Postigo, A. A., Zhang, S. H., and Dean, D. C. Cell anchorage regulates apoptosis through the retinoblastoma tumor suppressor /E2F pathway. J. Biol. Chem. 272, 8125-8128, 1997

Wayne State University
School of Medicine

Department of Pathology
Gordon H. Scott Hall
of Basic Medical Sciences
540 East Canfield Avenue
Detroit, Michigan 48201

Hyeong-Reh C. Kim, Ph.D.
Assistant Professor
313-577-2407 (office)
313-577-0193 (lab)
313-577-0057 (fax)

To whom it may concern;

A Career Development Award from the Department of the Army Breast Cancer Program has been extremely helpful for me to develop research career at Wayne State University. As presented in the body of report, we believe that we have made a significant progress during the first funding period. As you may know, the CDA does not support research expense and now it is difficult to continue to perform the proposed study which includes animal experiments. Thus, I would like to request research support of $ 127,829. The detailed budget and justification are included. I greatly appreciate for your consideration. I am looking forward to hearing from you. Thank you very much.

Sincerely,
9-24-97
Hyeong-Reh Choi Kim, Ph.D.

Anna Spiroff 9/24/97
Official of the Institution

1. DETAILED COST ESTIMATE

LABOR COST

Principal Investigator/Program Director (Last, first): Kim, Hyeong-Reh

DETAILED BUDGET FOR INITIAL BUDGET PERIOD DIRECT COSTS ONLY				FROM 1-Feb-98		THROUGH 31-Jul-98	
PERSONNEL (Applicant organization only)					DOLLAR AMOUNT REQUESTED (omit cents)		
NAME	ROLE ON PROJECT	TYPE APPT. (months)	% EFFORT ON PROJ.	INST. BASE SALARY	SALARY REQUESTED	FRINGE BENEFITS	TOTALS
Kim, Hyeong-Reh	Principal Invest.	12	40 %				
Rahman, Kazi	Research Assistan	12	50%	$24,700	$6,175	$1,408	$7,583
SUBTOTALS---------->					$6,175	$1,408	$7,583

EQUIPMENT

MATERIAL, SUPPLIES, AND CONSUMABLES

Purchase mice, 1,406: Animal Maintenance, 4,457;
Tissue culture reagents, 1,500; Molecular Biology Reagents, 1,500

$8,863

SUBCONTRACTS OR SUBGRANTS

DIRECT COSTS

INDIRECT COSTS

Total--------->

TRAVEL COSTS

PUBLICATION AND REPORT COSTS

CONSULTANT COSTS

OTHER DIRECT COSTS

FIXED FEE

DIRECT COSTS FOR INITIAL BUDGET PERIOD	$16,446
INDIRECT COSTS FOR INITIAL BUDGET PERIOD	$8,223
TOTAL COSTS	$24,669

Principal Investigator/Program Director (Last, first, middle): Kim, Hyeong-Reh

BUDGET FOR ENTIRE PROPOSED PROJECT PERIOD
DIRECT COSTS ONLY

BUDGET CATEGORY TOTALS	INITIAL BUDGET PERIOD	ADDITIONAL YEARS OF SUPPORT REQUESTED		
	6 Mos. of YR 2	YR 3	YR 4	
LABOR COSTS *Salaries and Fringe Benefits*	$7,583	$15,621	$16,090	
MAJOR EQUIPMENT				
SUPPLIES AND CONSUMABLES	$8,863	$18,257	$18,805	
SUBCONTRACTS OR SUBGRANTS				
TRAVEL				
PUBLICATION AND REPORT COSTS				
CONSULTANT COSTS				
OTHER DIRECT COSTS				
FIXED FEE				
TOTAL DIRECT COSTS	$16,446	$33,878	$34,895	
INDIRECT COSTS	$8,223	$16,939	$17,448	
TOTAL COSTS	$24,669	$50,817	$52,343	
TOTAL COSTS FOR ENTIRE PROPOSED PROJECT PERIOD			---------->	$127,829

BUDGET JUSTIFICATION

Budget Justification

Funding period of CDA (DAMD17-96-1-6181): 8/1/96-7/31-00

Research Support Requested: Yr. 2: 2/1/98 to 7/31/98
Yr. 3: 8/1/98 to 7/31/99
Yr. 4: 8/1/99 to 7/31/00

Personnel

Hyeong-Reh Choi Kim, Ph.D.
Role on Project: P.I.
Additional Salary requested: none
P.I. will be responsible for the entire project and personnel. She will design, supervise and perform the experiments.

Kazi H. Rahman, M.S.
Role on Project: Research Assistant
Salary requested 50%
Mr. Rahman will assist P.I. to perform experiments including western and northern blotting, kinase assay and animal experiments.

Supplies

$7030 to purchase 185 mice ($38.00 x 185); $2812/yr
$22,285 for animal maintenance for 2.5 years (4-8 animals/cage); $1.32 per cage/day

Tissue Culture Reagents (to purchase media, serum, growth factors to supplement MCF10A media, plasticwares): $3,000/yr
Molecular Biology Reagents (to purchase antibodies, Rb substrates, H1 substrates, radioisotope, immunostaining kits): $3,000/yr

Data management

The four treatment conditions, MCF10ATG3B cells with and without radiation (2 conditions) and bcl-2 overexpressing MCF10ATG3B cells with and without radiation (2 conditions), with at least 36 animals in each group, will be compared using the incidence of carcinoma (significant increase of incidence of invasive carcinoma from 25 % to at least 40 %) at the end of the experiment. A chi-square test for independence (equality of the proportion of mice with carcinoma) will be used to identify any significant differences among the groups. The overall chi-square test is expected to have a power of 90% against an alternative where the proportion of lesions that are carcinoma is 0.25 in the control group and this proportion is at least 0.40 in the remaining three groups.

An conservative significance of 0.01 for this experiment was selected to adjust for three comparisons (Bonferroni's technique would suggest a significance level of 0.013 for three comparisons). The three comparisons that are planned are: MCF10AT3 cells without radiation and bcl-2 overexpressing MCF10AT3 cells without radiation (experimental goal 1), MCF10AT3 cells without radiation and MCF10AT3 cells with radiation (experimental goal 2), and bcl-2 overexpressing MCF10AT3 cells without radiation and bcl-2 overexpressing MCF10AT3 cells with radiation (experimental goal 3).

Our evaluation of the four groups will also include differences between the four groups using characteristics of the lesions (histology) as well as parameters related to disruption of the basement membrane and metastatic ability. Categorical methods will be used for the ordinal variables and analysis of variance for continuous variables. In addition to characteristics of

lesions, we will evaluate the rate of change in the sizes of the tumors (diameter) using regression analysis.

40 mice will be used to examine the transforming ability of control and bcl-2 overexpressing MCF10ATG3B cells with or without irradiation *in vitro* (as proposed in the specific aim 2 in the original application)

Galectin-3 : A Novel Anti-Apoptotic Molecule with A Functional BH1 (NWGR) Domain of Bcl-2 Family

Shiro Akahani, Pratima Nangia-Makker, Hidenori Inohara[‡], Hyeong-Reh Choi Kim[†] and Avraham Raz[¶]

Tumor Progression and Metastasis Program, Karmanos Cancer Institute

Department of Pathology[†] and Radiation Oncology, Wayne State University,

School of Medicine, Detroit, MI 48201, U.S.A.

‡ Present Address: Department of Otolaryngology, Osaka University Medical School, 2-2 Yamadaoka, Suita, Osaka 565, Japan

¶ To whom correspondence should be addressed: Tumor Progression and Metastasis, Karmanos Cancer Institute, 110 East Warren Avenue, Detroit, MI 48201, U.S.A.

Phone (313)833-0960; FAX (313)831-7518

Abstract

Galectin-3, a β-galactoside-binding protein, has been shown to be involved in tumor progression and metastasis. Here, we demonstrate that expression of galectin-3 in human breast carcinoma BT549 cells inhibits cisplatin (CDDP)-induced Poly (ADP-ribose) polymerase (PARP) degradation and apoptosis, without altering Bcl-2, Bcl-X_L or Bax expressions. Galectin-3 contains the NWGR amino acid sequence conserved in the BH1 domain of *bcl-2* gene family and a substitution of glycine to alanine in this motif abrogated its anti-apoptotic activity. Our findings demonstrate that galectin-3 inhibits apoptosis through a cysteine protease pathway and highlight the functional significance of the NWGR motif in apoptosis resistance of non-Bcl-2 protein.

A number of antineoplastic agents have been developed for the eradication of malignancies but successful chemotherapy still depends on the control of multidrug resistance since failure may lead to mortality. For example, *cis*-Platinum (II) Diammine Dichloride (CDDP), a potent anticancer compound, which functions through interstrand DNA crosslinks and the induction of apoptosis (1), has improved the outcome of many cancers, but the mechanism(s) of CDDP resistance remains to be defined.

Expression of galectin-3, a *Mr* 31 kDa carbohydrate-binding protein (2), correlates with clinicopathological features in head and neck cancer (3), thyroid cancer (4), gastric cancer (5), and colon cancer (6). In several experimental tumor systems galectin-3 expression is related to the metastatic potential (7,8). Recently it has been suggested that galectin-3 may inhibit apoptosis through interactions with complementary carbohydrates (9) or with the anti-apoptotic protein, Bcl-2 (10). Galectin-1 and -9 have been reported to induce apoptosis (11), suggesting that some members of the galectin family are involved in the regulation of apoptosis. Moreover, a domain in the carboxy-terminus of galectin-3 was found to have a significant sequence similarity with the BH1 domain of the Bcl-2 family of proteins containing the NWGR motif (10), which is responsible for the anti-apoptotic activity of Bcl-2. Further investigation was thus prompted to establish a possible role of galectin-3 in the mechanism of drug-induced apoptosis. To this end we have used the recently identified galectin-3 null cells, i.e., the human breast carcinoma BT549 cells.

In this study we demonstrate that expression of galectin-3 in human breast carcinoma BT549 cells inhibits CDDP-induced Poly (ADP-ribose) polymerase (PARP) degradation and apoptosis, and that the NWGR motif of galectin-3 is required for its anti-apoptotic activity, as determined by analysis of a mutagenesis study showing that an amino-acid substitution of glycine to alanine at position 182 abrogates its function.

Human breast carcinoma BT549 cell clones transfected with plasmid DNA containing inserts in either the sense (11811, 11913, 11914) or the antisense control (41421) orientation encoding human galectin-3 were established from the galectin-3 null parental cells as previously reported (8). Here we confirmed galectin-3 expression in the parental BT549 cells, and its clones 41421 and

11914 by Western blot analysis. Only sense transfected clones such as 11914 cells expressed galectin-3, while the other two cell types remained galectin-3 null (Fig.1A).

To test the effect of galectin-3 expression in CDDP-induced cytotoxicity, we treated all clones with or without CDDP (12), and cell viabilities were subsequently evaluated by trypan blue dye exclusion test. After an exposure to 25μM CDDP, cell death was predominantly observed in parental BT549 and 41421 cells when compared with 11811, 11913 and 11914 cells (Fig.1B). Parental BT549 and 41421 cells showed similar sensitivity to CDDP treatment ; A 72 hour exposure to CDDP exhibited a decrease in viability to less than 30% of the parental BT549 and 41421 cells, while more than 60% of all galectin-3 expressing clones remained viable even after a 72 hour exposure with the same CDDP concentration.

To assess whether CDDP-treated cells underwent apoptosis, cells were stained with the DNA binding dye (propidium iodide) and subjected to flow cytometric DNA analysis. The apoptotic subpopulation can be detected as the appearance of a discrete peak and increased fluorescence in sub-G_1 cell cycle region in the DNA histogram. It has been shown that the sub-G_1 peak derives from cells in G_0/G_1 region which undergo apoptosis, and a decrease in G_0/G_1 DNA content results from partial digestion or modification during apoptosis (13). Sub-G_1 population of the galectin-3 null parental BT549 and 41421 cells occupied greater than 30% of the DNA histogram after a 72 hour exposure to a concentration of 25μM of CDDP, while that of 11914 cells occupied not more than 20% (Fig.2D,2E,2F). To further investigate apoptotic features including nuclear condensation and fragmentation, CDDP-treated cells were visualized by fluorescence microscopy following paraformaldehyde fixation and staining with the DNA-binding fluorochrome bis (benzimide) trihydrochloride (Hoechst 33258). This procedure revealed the presence of fragmentated as well as abnormally-shaped condensed chromatin both of which are characteristic of apoptosis. As shown in Fig.2G, 2H, and 2I, death in all three types of cells involved apoptosis. More than 40% of CDDP-treated parental BT549 cells exhibited nuclear morphologies which are indicative of apoptosis : DNA fragmentation and condensed chromatin (Fig.2G). Similar patterns of chromatin condensation and nuclear fragmentation were seen in CDDP-treated 41421 cells (Fig.2H). However, CDDP-

treated 11914 cells were morphologically different from that of the other two cell types : more visible nucleoli mostly without altered chromatin structure (Fig.2I). When considered together with the result of flow cytometry, apoptosis was largely observed in galectin-3 null parental BT549 and 41421 cells, yet largely absent in galectin-3 expressing 11914 cells.

We further evaluated whether expression of galectin-3 in BT549 cells resulted in altered expression of the Bcl-2 family of proteins since previous studies had revealed that an elevated Bcl-2 level influenced the cell survival effect (16). Galectin-3 null and positive cell clones showed no difference in the level of Bcl-2 expressions (Fig.1A), and likewise no significant difference in the level of the Bcl-X_L and Bax expressions among these three cell clones was observed (data not shown). These expressions were not altered by a 72 hour exposure to 25μM CDDP (data not shown). We then questioned the possibility that galectin-3 might regulate apoptosis through interactions with members of the Bcl-2 family of proteins, but a complex formation between galectin-3 and Bcl-2 or Bax in 11914 cells could not be established by co-immunprecipitation assay (data not shown).

PARP is a substrate for mammalian cell death proteases and is degraded by activated cysteine proteases of the interleukin-1β converting enzyme (ICE)/*ced-3* family including CPP32/Yama (caspase-3)(14,15). Degradation of PARP is a characteristic feature of the early stage of apoptosis and leads to inhibition of DNA repair, activation of an endonuclease, and eventually to cell death (17). To further study the involvement of galectin-3 in the apoptosis pathway, we examined expressions of intact and cleaved PARP before and after a 72 hour exposure to CDDP, showing that CDDP induced the cleavage of intact PARP (116 kDa) into the inactive fragment (85 kDa) in galectin-3 null parental BT549 and 41421 cells but not in galectin-3 expressing 11914 cells (Fig.3). Interestingly, the levels of precursor CPP32/Yama in parental BT549 and 41421 cells attenuated after a 72 hour exposure to CDDP, when compared to expression in 11914 cells. This suggests activation of CPP32/Yama in galectin-3 null parental BT549 and 41421 cells manifested itself as an active form of 20 kDa.

The human proto-oncogene *bcl-2* and the *Caenorhabditis elegans* gene *ced-9*, both of which

protect cells from apoptosis (18), are classified in the same gene family (19). Previous reports demonstrated that a substitution of glycine in the NWGR motif of Bcl-2 BH1 domain and its highly-conserved motif of ced-9 resulted in the loss of anti-apoptotic activity of Bcl-2 and its binding activity to Bax (20). The BH1 domain in the Bcl-2 family of proteins and its partial homology with the carboxy-terminus of galectin-3 indicate that the highly-conserved NWGR motif might be critical to the apoptotic function of galectin-3 (Fig.4A). To determine the significance of the NWGR motif in galectin-3, mutant galectin-3 (glycine 182 to alanine) was generated by PCR-mediated site-directed mutagenesis techniques. Three stable transfectants showed differences in expression of mutant galectin-3; clone 5 expressed mutant galectin-3 at the highest level (most among the three) and its expression was as strong as that of the wildtype 11914 cells (Fig.4B). Simultaneously we examined the expression of Bcl-2, but no alteration in Bcl-2 expression was detected following the introduction of mutant galectin-3 (data not shown). To evaluate its function in CDDP-induced apoptosis, we treated three stable clones with 25μM CDDP for 72 hours, and time-dependent cell viability of clones expressing mutant galectin-3 with CDDP treatment was assessed and compared with parental and the galectin-3 wildtype transfected BT549 cells (Fig.4C). Three clones and parental BT549 cells revealed a similar sensitivity to CDDP, with clone 5 demonstrating the most susceptibility to CDDP among the clones. Next, we stained CDDP-treated cell clones with propidium iodide for the analysis of sub-G_1 content in DNA histogram, and with Hoechst 33258 for the assessment of chromatin condensation and fragmentation. All galectin-3 mutant clones displayed similar features of apoptosis as observed in parental BT549 and 41421 cells (data not shown). In addition, all of the galectin-3 mutant clones underwent activation of CPP32/Yama and proteolytic cleavage of PARP after 72 hours of CDDP exposure (Fig.5). Taken together, these findings indicate that introduction of mutant galectin-3 resulted in failure to inhibit CDDP-induced apoptosis in BT549 cells, and that the NWGR motif of galectin-3 is critical for its anti-apoptotic function as of Bcl-2 protein.

The results indicate galectin-3 confers apoptosis resistance to CDDP in a cysteine protease dependent manner, similarly to Bcl-2 (15). It remains possible that galectin-3 can replace or mimic

Bcl-2 leading to the inhibition of CDDP-induced apoptosis involving CPP32/Yama protease activation and PARP degradation.

Mutagenesis studies revealed that like Bcl-2 or ced-9, galectin-3 regulates its anti-apoptotic activity through the glycine residue of the NWGR motif. It has been previously demonstrated that synthetic glycoamines or glycosylated molecules such as Mac-2 binding protein could regulate homotypic aggregation through their interactions with galectin-3 (21), and it was suggested that the disruption of galectin-3-mediated cell-cell interactions on the cell surface resulted in induction of apoptosis in murine melanoma B16-F10 (9). The results from the carboxy-terminus mutation raises the possibility that substitution of the glycine residue may change the affinity to carbohydrates on the cell surface, block galectin-3 mediated cell-cell interaction, and cause the loss of anti-apoptotic function of galectin-3. However, our preliminary study showed that in parental BT549 cells, CDDP activity was not inhibited by exogenously added recombinant wildtype galectin-3 with a concentration of 10μg/ml. This finding indicates that the role of galectin-3 in apoptosis is more likely to involve a mechanism in the intracellular compartment rather than on the cell surface. It is now well accepted that the Bcl-2 is localized at the mitochondrial membrane and regulates apoptosis by blocking the effect of cytochrome c from it (22). However, galectin-3 was localized at nuclease, cytoplasm, cell surface or secreted, but not to the golgi apparatus or the mitochondria. This suggests that the two proteins regulate their anti-apoptotic activities at different cellular compartments.

It should be emphasized that galectin-3 does not belong to the Bcl-2 gene family since they share less than 30% homology (10). However, whether or not they have merged from a common ancestral gene containing the NWGR motif remains unknown, and it should be noted that among the galectin family of proteins only galectin-3 contains the Bcl-2 NWGR motif. In summary, we show here that galectin-3 is a novel anti-apoptotic molecule, which like Bcl-2 acts through cysteine protease pathways, this finding may lead to the development of new reagents to overcome tumor cells' multi-drug resistance, and contribute to the understanding of the role of galectin-3 in metastasis.

Figure Legend

Figure 1.

(A) Galectin-3 and Bcl-2 expressions in untreated BT549 cells and transfectants. Western blot analysis: 5×10^6 cells were pelleted by centrifugation, washed with calcium-magnesium free phosphate buffered saline (CMF-PBS) pH 7.4, and subsequently lysed in 1ml reducing SDS-polyacrylamide gel electrophoresis (PAGE) sample buffer (2% SDS, 62.5mM Tris-HCl pH 6.8, 10% glycerol, 5% β-mercaptoethanol). Then cell lysates were agitated overnight at room temperature, and stored at -70°C until use. For Western blot analyses, approximately 20μg of total proteins were boiled for 5min, separated on reducing 15% SDS-PAGE and blotted onto a nitrocellulose membrane. Blots were probed with rat anti-galectin-3 (American Type Culture Collection, Rockville, MD) or mouse anti-Bcl-2 antibody (Dako, Carpinteria, CA) according to the ECL (Amersham, Buckinghamshire, England)-Western procedure. Human breast carcinoma MCF-7 and lymphoma WSU-CLL were used as positive controls of galectin-3 and Bcl-2, respectively. These results were representative of three separate experiments. Galectin-3 and Bcl-2 expressions in untreated cells were also confirmed by Northern blot analyses (data not shown).

(B) Cell viability of parental BT549 (—■—), antisense transfectant 41421 (—▲—), and sense transfectants 11811 (—△—), 11913 (—▽—) and 11914 (—▼—) cells with 25μM CDDP treatment in time-dependent manner. Cells were cultured with or without CDDP (12), and harvested as previously described (24), and cell viability was determined using trypan blue dye exclusion test. Data are the mean ± s.d. of triplicate determinations from three separate experiments.

Figure 2.

Flow cytometric cell cycle histograms of ethanol-fixed parental BT549 and transfectants stained with 50μg/ml propidium iodide before [parental BT549 (A), 41421 (B), 11914 (C)] and after

treatment with 25μM CDDP for 72 hours [parental BT549 (D), 41421 (E), 11914 (F)] (13). Cells with or without CDDP treatment were fixed with 80% ethanol at 4°C for 30min, washed with CMF-PBS pH7.4, and resuspended with 50μg/ml propidium iodide (Coulter Immunology, Hialeah, FL)diluted with CMF-PBS pH7.4 containing 0.1% Triton X-100, 0.1mM EDTA pH8.0, and 50μg/ml RNase A. Then samples were agitated at 4°C for not less than 15min prior to analysis with flow cytometry. Asterisk represents cells in the sub-G_1 region that have undergone chromatin degradation associated with apoptosis.

Morphological changes associated with apoptosis in parental BT549 cells (G) and tranfectants [41421(H), 11914 (I)] treated with 25μM CDDP for 72 hours. Briefly, 1×10^6 of CDDP-treated cell pellets were collected by centrifugation at 2000rpm for 5min, and fixed with 3% paraformaldehyde at room temperature for 10min. Then cells were washed with CMF-PBS pH7.4, and stained dark with 8μg/ml Hoechst 33258 in CMF-PBS pH7.4 at room temperature for 15min. Samples were loaded on the glass-slide coated with 3-aminopropyl-trimethoxysilane (Sigma, St. Louis, MO), and chromatin fragmentation as well as its condensation in apoptotic cells were observed through fluorescence microscopy with UV filter (25).

Figure 3.

Cleavage of the DNA repair enzyme, PARP and precursor CPP32/Yama expressions in parental BT549 cells and transfectants exposed to CDDP. Before and after the treatment with 25μM CDDP for 72 hours, proteins from cell lysates were electrophoresed on reducing 8% or 15% SDS-PAGE, transferred to nitrocellulose, and probed with mouse anti-PARP antibody (Biomol Research Meeting, PA) or goat anti-CPP32/Yama antibody (Santa Cruz Biotech, Santa Cruz, CA), respectively. The amount of protein used was same as described in Fig.1A.

Figure 4.

Stable clones expressing mutant galectin-3 and comparison with parental BT549 cells and transfectants of galectin-3 cDNA. (A) Schematic representation of the BH1 domain and its similarity with carbohydrate-binding domain of galectin-3. The NWGR motif which is responsible for anti-apoptotic function of Bcl-2 was marked by bold. An amino-acid substitution of glycine 182 to alanine is shown in the bottom row. (B) Western blot analysis: Galectin-3 with an amino-acid substitution of 182 glycine for alanine was established by following the protocol of *in vitro* site-directed mutagenesis kit (Stratagene, La Jolla, CA), and tranfected into parental BT549 cells (26). Oligonucleotide primers for PCR were sense (5'-TGGATAATAACTGGGCAAGGGAAGAAAG-3') and antisense (5'-CTTTCTTCCCTTGCCCAGTTATTATCCA-3') encoding 548-575 nucleotides in human galectin-3 cDNA. Mutant galectin-3 in stable clones were detected using rat anti-galectin-3 as shown in Fig.1A.

(C) Cell viability of clones expressing mutant galectin-3 (—♦— : clone #1, —•— : clone #3, —□— : clone #5) with 25μM CDDP treatment in time-dependent manner and comparison with parental BT549 (—▪—) and wildtype galectin-3 transfectant 11914 cells (12). Viability was determined as described in Fig.2 (24).

Figure 5.

Cleavage of PARP and precursor CPP32/Yama expressions in BT549 tranfectants of mutant galectin-3 cDNA. Before and after 72 hours exposure to 25μM CDDP, cleavage of PARP and CPP32/Yama in transfectants was examined by Western blot as described in Fig.3.

References

1. A.E. Cress and W.E. Dalton, *Cancer Metastasis Rev.* **15,** 499 (1996)
2. S.H. Barondes, et al., *Cell* **76,** 597 (1994)
3. A. Gillenwater, X-C. Xu,, A.K. El-Naggar, G.L. Clayman, R. Lotan, *Head and Neck* **18,** 422 (1996)
4. X-C. Xu,, A.K. El-Naggar, R. Lotan, *Am. J. Pathol.* **147,** 815 (1995)
5. R. Lotan, et al., *Int. J. Cancer* **56,** 474 (1994)
6. H.L. Schoeppner, A. Raz, S.B. Ho, R.S. Bresalier, *Cancer* **75,** 2818 (1995)
7. A. Raz, et al., *Int. J. Cancer* **46,** 871 (1990)
8. P. Nangia-Makker, E. Thompson, C. Hogan, J. Ochieng, A. Raz, *Int. J. Oncol.* **7,** 1079 (1995)
9. G.V. Glinsky and V.V. Glinsky, *Cancer Lett.* **101,** 43 (1996)
10. R.Y.Yang, D.K. Hsu, F-T Liu, *Proc. Natl. Acad. Sci. USA.* **93,** 6737 (1996)
11. N.L. Perillo, K.E. Pace, J.J. Seilhamer, L.G. Baum, *Nature* **378,** 736 (1995)

    N.L. Perillo, C.H. Uittenbogaart, J.T. Nguyen, L.G. Baum, *J. Exp Med* **185**, 1851 (1997)

    J. Wada, K. Ota, A. Kumar, E.I. Wallner, Y.S. Kanwar, *J. Clin. Invest.* **99**, 2452 (1997)
12. One million cells were cultured overnight at 37°C in Dulbecco's modified Eagle's medium (Gibco BRL, Grand Island, NY) supplemented with 10% heat-inactivated fetal bovine serum, 2mM glutamine, non-essential amino acids and antibiotics (Gibco BRL, Grand Island, NY)(10% complete DMEM). Next day cells were washed twice with CMF-PBS and replaced with 10% complete DMEM containing 25mM CDDP. Then cells were cultured further for the indicated times.
13. W.G. Telford, L.E. King, P.J. Fraker, *Cytometry* **13,** 137 (1992)
14. M. Tewari, et al., *Cell* **81**, 801 (1995)
15. A.M. Ibrado, Y. Huang, G. Fang, L. Liu, K. Bhalla, *Cancer Res.* **56,** 4743 (1996)
16. S.J. Korsmeyer, *Trends in Genetics* **11,** 101 (1995)

    Z. Zhang, K. Vuori, J.C. Reed, E. Ruoslahti, *Proc. Natl. Acad. Sci. USA* **92,** 6161 (1995)

17. S.H. Kaufman, S. Desnoyers, Y. Ottaviano, N.E. Davidson, G.G. Poirier, *Cancer Res.* **53,** 3976 (1993)

18. J.C. Reed, *J. Cell Biol.* **124,** 1 (1994)

A. Fraser, G. Evan, *Cell* **85,** 781 (1996)

19. M.O. Hengartner, and H.R. Horvitz, *Cell* **76,** 665 (1994)

20. M.O. Hengartner, and H.R. Horvitz, *Nature* **369,** 318 (1994)

X.M. Yin, Z.N. Oltvali, S.J. Korsmeyer, *Nature* **369**, 321 (1994)

21. G.V. Glinsky, V.V. Mossine, J.E.Price, D. Bielenberg, V.V. Glinsky, *Clin. & Exp. Metastasis* **14,** 253 (1996)

H. Inohara, S. Akahani, K. Koths, A. Raz, *Cancer Res.* **56**, 4530 (1996)

22. J. Yang, et al., *Science* **275,** 1129 (1997)

R.M. Kluck, E. Bossy-Wetzel, D.R. Green, D.D. Newmeyer, *Science* **275**, 1132 (1997)

23. A.M. Chinnaiyan, et al., *J. Biol. Chem.* **271,** 4573 (1996)

24. R.A. Huddart, J. Titley, G.T. Robertson, A. Horwich, C.S. Cooper, *Euro. J. Cancer* **31A,** 739 (1995)

25. F. Oberhammer, et al., *EMBO J.* **12,** 3679 (1993)

26. Mutant galectin-3 (glycine 182 to alanine) cDNA was cloned into the *EcoRI* site of the pCNC10 vector. For transfection, 2μg plasmid DNA was isolated and incubated with 10μl lipofectamine (Gibco BRL, Grand Island, NY), and this mixture was added onto the cells grown to 70% confluency. Clones were selected at random using 800μg/ml G418 (Gibco BRL, Grand Island, NY) and maintained in 10% complete DMEM containing 400μg/ml G418.

27. We thank E.W. Thompson for providing us with BT549 cell line; F.G. Kern for the pCNC10 vector ; E. Van Buren, R. Johnson, and L. Tait for the flowcytometry analyses; V. Powell for typing and editing and Drs.W. Wei and R. Bright for their critical evaluation of the manuscript. Supported by U.S.Army grant DAMD 17-96-1-6181, NIH grant R29-CA64139 (H.-R.C.K.), R01-CA46120 and the Paul Zuckerman Support Foundation for Cancer Research (A.R.).

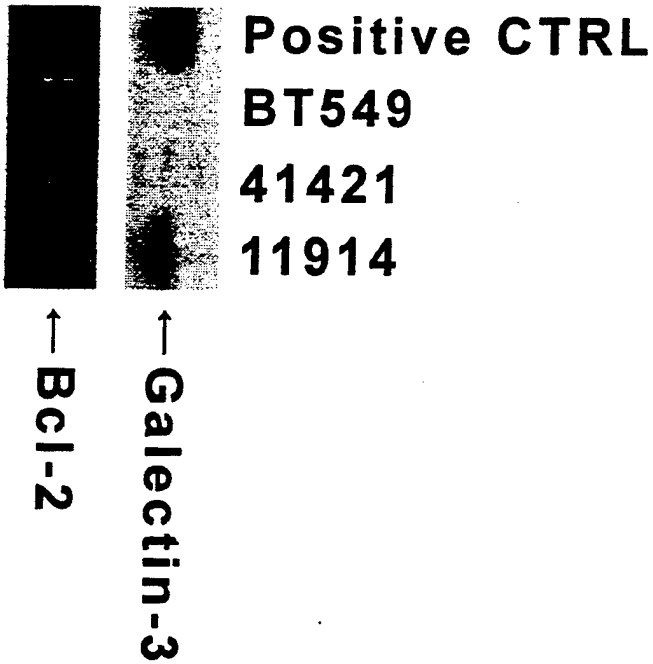

Figure 1A

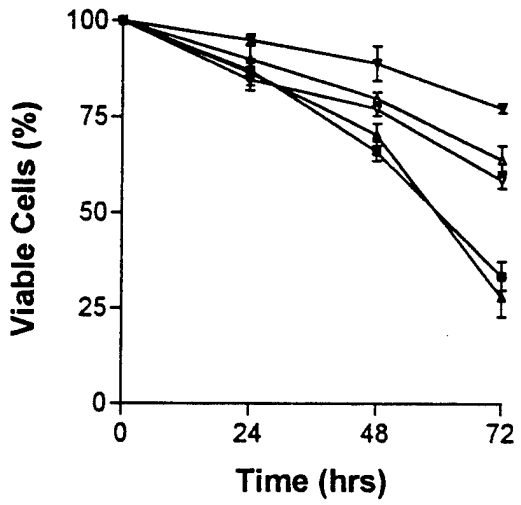

Figure 1B

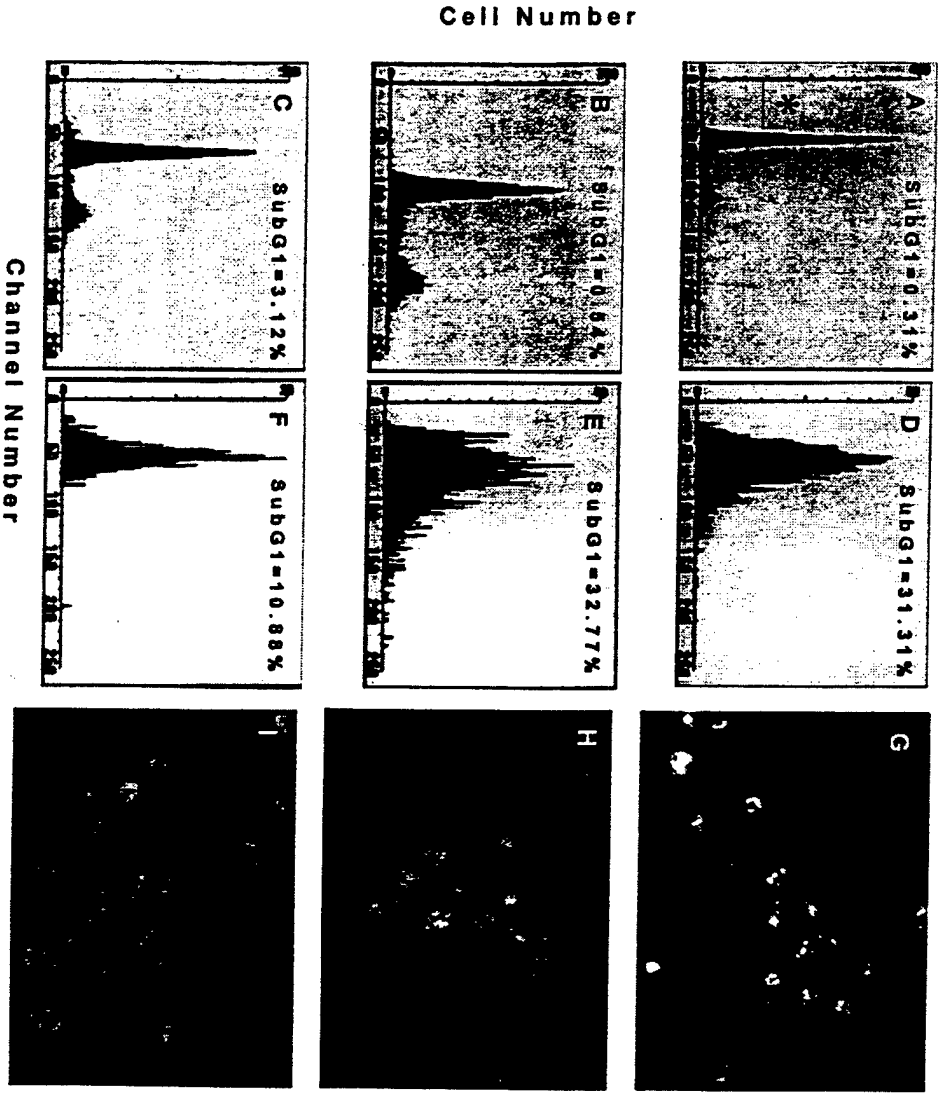
A
SubG1=0.31%
B
SubG1=0.54%
C
SubG1=3.12%
D
SubG1=31.31%
E
SubG1=32.77%
F
SubG1=10.88%
G
H
I
Cell Number
Channel Number

Figure 2

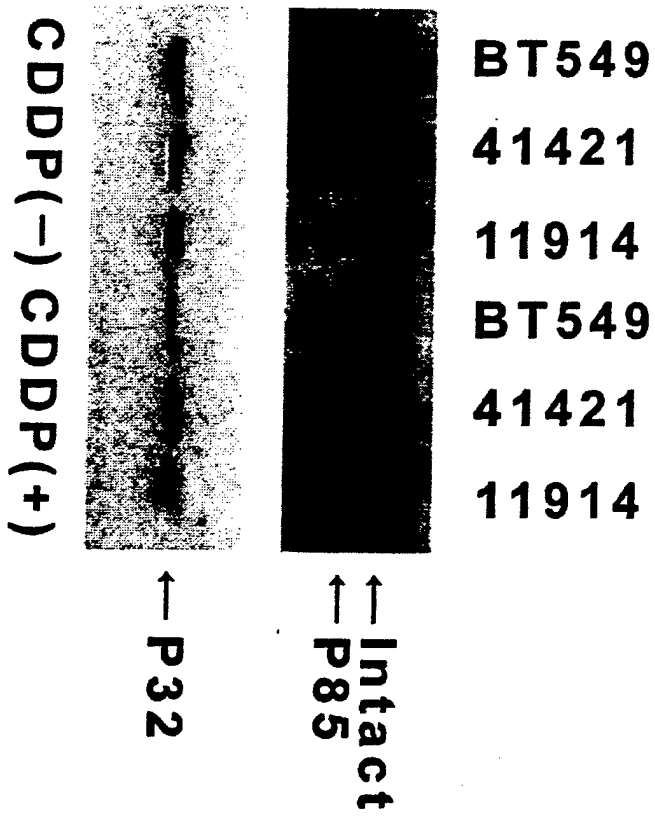
BT549
41421
11914
BT549
41421
11914
Intact
P85
P32
CDDP(−) CDDP(+)

Figure 3

Bcl-2	136	ELFRDGV-**NWGR**IVAFFEFGG	155
Bax	98	DMFSDGNF**NWGR**VVALFYFAS	118
Bcl-XL	150	ELFRDGV-**NWGR**IVAFFSFGG	169
Galectin-3	174	NTKLD-N-**NWGR**E----ERQS	188
		↕	
Galectin-3/$G_{182}A$		**A**	

Figure 4A

BT549

41421

11914

BT549/Gal-3G182 A#1

41421 /Gal-3G182 A#3

11914 /Gal-3G182 A#5

←Galectin-3

Figure 4B

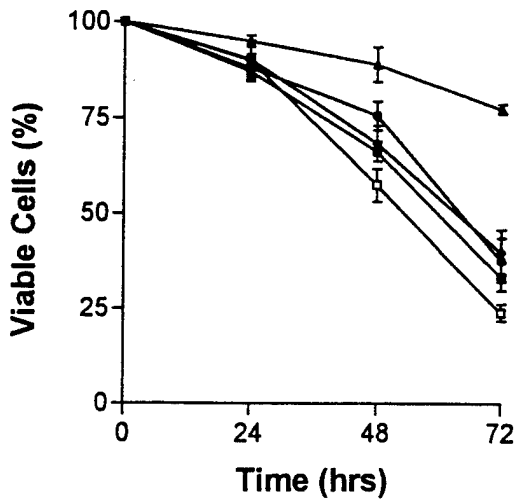

Figure 4C

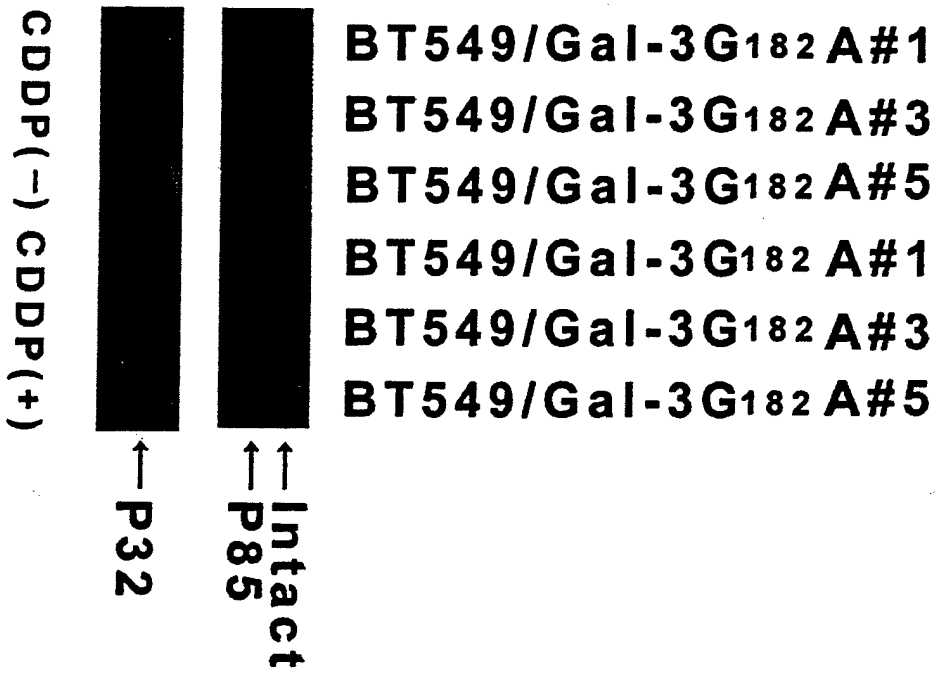
BT549/Gal-3G182A#1
BT549/Gal-3G182A#3
BT549/Gal-3G182A#5
BT549/Gal-3G182A#1
BT549/Gal-3G182A#3
BT549/Gal-3G182A#5
Intact
P85
P32
CDDP(−) CDDP(+)

Figure 5

INTERNATIONAL JOURNAL OF ONCOLOGY 11: 0-00, 1997

Levels of p21$^{WAF1/CIP1}$ do not affect radiation-induced cell death in human breast epithelial cells

HYEONG-REH CHOI KIM[1,2], GANGYONG LI[1], HAROLD E. KIM[2], SUE J. HAN[3], KAZI H. RAHMAN[1], HAO LIU[1], DAVID WAID[2] and YONG J. LEE[4]

[1]Department of Pathology, [2]Department of Radiation Oncology, Wayne State University School of Medicine, and Karmanos Cancer Institute, Detroit, MI 48201; [3]Department of Radiation Oncology, Veterans Administration Medical Center, Detroit, MI 48201; [4]Department of Radiation Oncology, William Beaumont Hospital, Royal Oak, MI 48073, USA

Abstract. Loss of the wild-type p53 activity and/or overexpression of the proto-oncogene *bcl*-2 are frequently detected in breast cancer and suggested to be related to chemotherapy and radiation therapy resistance. To identify the downstream signaling molecules for anti-proliferative and apoptotic activities of p53 and to investigate the interaction of *bcl*-2 with p53 in human breast epithelial cells, we have used the MCF10A cell line. We previously showed that overexpression of *bcl*-2 downregulates expression of p21$^{WAF1/CIP1}$ (a cyclin dependent kinase inhibitor which mediates p53 dependent G_1 arrest) and suppresses DNA damage-induced apoptosis in MCF10A cells. In the present study, we constitutively overexpressed p21$^{WAF1/CIP1}$ in *bcl*-2 overexpressing MCF10A cells to determine whether downregulation of p21$^{WAF1/CIP1}$ is necessary for the anti apoptotic activity of *bcl*-2, and to investigate the roles of p21$^{WAF1/CIP1}$ in p53-mediated cell death upon irradiation. Overexpression of p21$^{WAF1/CIP1}$ resulted in growth inhibition, but had no effect on *bcl*-2 inhibition of apoptosis following irradiation. Also, overexpression of p21$^{WAF1/CIP1}$ did not affect the dose-dependent radiation-induced cell lethality as determined by a clonogenic survival assay. These results suggest that *bcl*-2 downregulation of p21$^{WAF1/CIP1}$ is independent of the anti-apoptotic activity of *bcl*-2, and that p21$^{WAF1/CIP1}$ is not involved in the p53-mediated cell death pathway.

Introduction

One of the most frequent genetic defects in human cancer is loss of the wild-type activity of the tumor suppressor gene p53 (1). Hoping to rescue anti-oncogenic and apoptotic activities of p53 in tumor cells, efforts have been made to identify p53-downstream signaling molecules. Since p21$^{WAF1/CIP1}$ was identified as a p53 inducible gene (WAF1) (2), independently as an inhibitor of cyclin-dependent kinases (CIP1) (3,4) and also as a gene which is differentially expressed during cellular senescence (SDI1) (5), it has been in demand to determine the roles of p21$^{WAF1/CIP1}$ in the p53 pathways. The deletion of the p21$^{WAF1/CIP1}$ gene in a human colon carcinoma cell line results in complete loss of G_1 arrest following DNA damage (6). In contrast, overexpression of p21$^{WAF1/CIP1}$ results in increases in the G_1 cell population, suppression of anchorage-independent growth and inhibition of tumor cell growth *in vitro* and in nude mice (2,7), clearly suggesting that p21$^{WAF1/CIP1}$ induces G_1 arrest and mediates anti-proliferative activity of p53. We have previously shown that expression of p21$^{WAF1/CIP1}$ is downregulated by overexpression of the anti-apoptotic gene *bcl*-2 in human breast epithelial cells (MCF10A cells) (8). In this study, we have investigated whether *bcl*-2 down-regulation of p21$^{WAF1/CIP1}$ is associated with *bcl*-2 inhibition of p53-mediated apoptosis following DNA damage. We also examined whether levels of p21$^{WAF1/CIP1}$ affect clonogenic survival of human breast epithelial cells upon irradiation.

Materials and methods

Transfection. The human p21$^{WAF1/CIP1}$ under the control of the SV-40 promoter (provided by Dr B. Vogelstein, Johns Hopkins University) together with hygromycin resistant vector were introduced into the pooled population of *bcl*-2 overexpressing MCF10A cells. Establishment and characterization of *bcl*-2 overexpressing MCF10A cells were previously reported (8). For transfection, $5x10^5$ cells were plated on a 100 mm dish. Next day, cells were washed with DMEM/F12 medium three times and overlaid with 5 ml of DMEM/F12 medium containing 15 μg of p21$^{WAF1/CIP1}$ expression vector, 5 μg of hygromycin resistant vector and 20 μl of lipofectin (Sigma, MO). Six to eight hours later, medium was replaced with regular MCF10A medium and cells were grown for 2 days. Transfectants were selected in the presence of 100 μg/ml hygromycin (Sigma, MO).

Correspondence to: Dr Hyeong-Reh Choi Kim, Department of Pathology, Wayne State University School of Medicine, and Karmanos Cancer Institute, Detroit, MI 48201, USA

Key words: radiation-induced cell death, p21$^{WAF1/CIP1}$, *bcl*-2, p53, human breast epithelial cells

Western blot analysis of p21$^{WAF1/CIP1}$. To prepare whole-cell lysates, exponentially growing cells were lysed using SDS sample buffer at a volume of 1x10^6 cells/50 µl. Protein concentration was measured using protein assay reagents (Pierce, IL). Cell extracts were boiled for 10 min and chilled on ice, subjected to SDS PAGE analysis, and then electrophoretically transferred to nitrocellulose membrane. Levels of p21$^{WAF1/CIP1}$ proteins were detected using anti-p21$^{WAF1/CIP1}$ antibody (Ab-1 from Oncogene Science, NY).

Nuclear staining. Cells were plated on coverslips in a 6-well plate. The next day, cells were irradiated at a dose rate of 2 Gy/min using a 6-MeV linear accelerator. One day after treatment, cells were washed with PBS and fixed with 4% paraformaldehyde in PBS for more than 12 h at 4°C. Cells were stained with 1 µg/ml bisBenzimide (Hoechst 33258) in PBS for 15 min at room temperature and washed with PBS. The cells were mounted in 0.1% phenylenediamine and 90% glycerol in PBS. Nuclear morphology was examined under UV illumination on a fluorescent microscope.

Western blot analysis of PARP. One million cells were plated on a T-75 flask. The next day, cells were irradiated on a Theratron 780, ^{60}Co teletherapy machine at a dose rate of 65 cGy/min. One day after irradiation, whole cell lysates were prepared from floating cells and adherent cells separately. Western blot analysis was performed as described above and cleavage of PARP protein was determined using anti-PARP antibody (C-2-10 form Biomol Research Lab, PA).

Cell survival determination. Cells were irradiated at room temperature with a GE Maximar 250-III orthovoltage X-ray unit (general Electric, Chicago, IL) at a dose rate of 1.17 Gy/min. The tube voltage was 250 kVp, current was 15 mA, and added filtration was 0.25 mm Cu. The radiation dose ranged from 0 to 8 Gy administered in a single fraction.

Two days prior to the experiment, cells were plated into T-25 flasks. After irradiation exposure, cells were trypsinized, counted, and appropriate dilutions were made. The appropriate number of cells were plated into two replicate T-25 flasks containing medium and feeder cells (irradiated with 25 Gy) which were prepared a day prior to the experiment. The number of feeder cells was adjusted so that a total of 1x10^5 cells (feeder cell plus the test cells) were plated. After 1-3 weeks of incubation at 37°C [8-9 days for control vector transfected cells (py3), 2-3 weeks for p21$^{WAF1/CIP1}$ transfected cells (clone #2 and pooled population)], colonies were stained and counted. All survival experiments were performed in triplicate or quadruplicate. Plating efficiencies for py3, p21 #2, p21-pp were 0.49, 0.47 and 0.46 respectively.

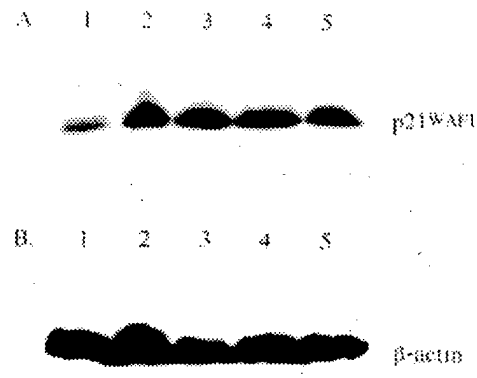

Figure 1. Western blot analysis of p21$^{WAF1/CIP1}$. A, The levels of p21 WAF1/CIP1 protein were determined in the control vector (py3) transfected *bcl*-2 overexpressing MCF10A cells (lane 1) and p21$^{WAF1/CIP1}$ transfected clones (lane 2, clone #2; lane 3, clone #4; lane 4, clone # 6; lane 5, pooled population). B, In order to confirm the amount of protein loaded in each lane, the same filter was reprobed with anti-ß-actin antibody.

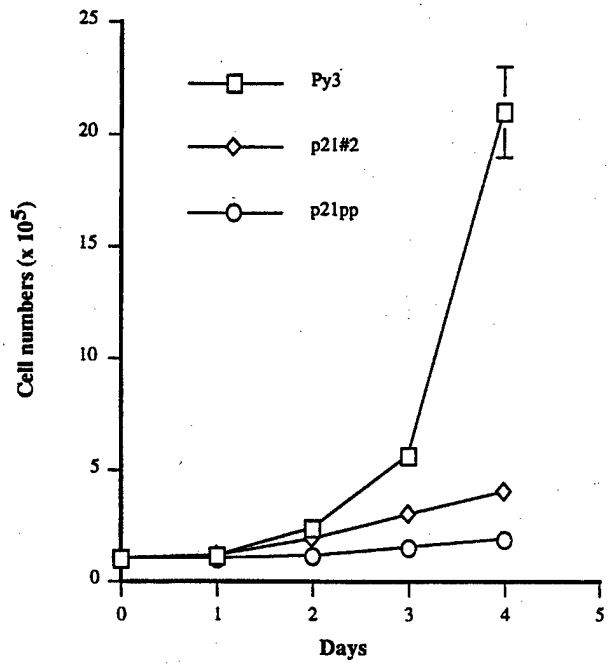

Figure 2. Effects of p21$^{WAF1/CIP1}$ overexpression on the growth rates. 1x10^5 cells were plated on 100-mm plates and cultured using MCF10A medium as previously described (8-10). Cell numbers were counted daily and mean values of triplicate are shown plotted against time. Error bars represent standard deviation of the mean of triplicate (error bars smaller than the size of symbols are not shown).

Results and Discussion

To elucidate the critical components in the p53-mediated signal transduction pathways and their roles in p53 mediated cell growth inhibition and cell death in breast epithelial cells, we used MCF10A cells. The MCF10A cell line is a spontaneously immortalized cell line that was derived from diploid human breast epithelial cells (9,10). Overexpression of the death suppressing gene *bcl*-2 in these cells resulted in downregulation of p21$^{WAF1/CIP1}$ expression and inhibition of apoptotic cell death (ref. 8; Fig. 3A and B, and Fig. 4). We have addressed the question of whether *bcl*-2 downregulation of p21$^{WAF1/CIP1}$ is necessary for *bcl*-2 inhibition of apoptosis

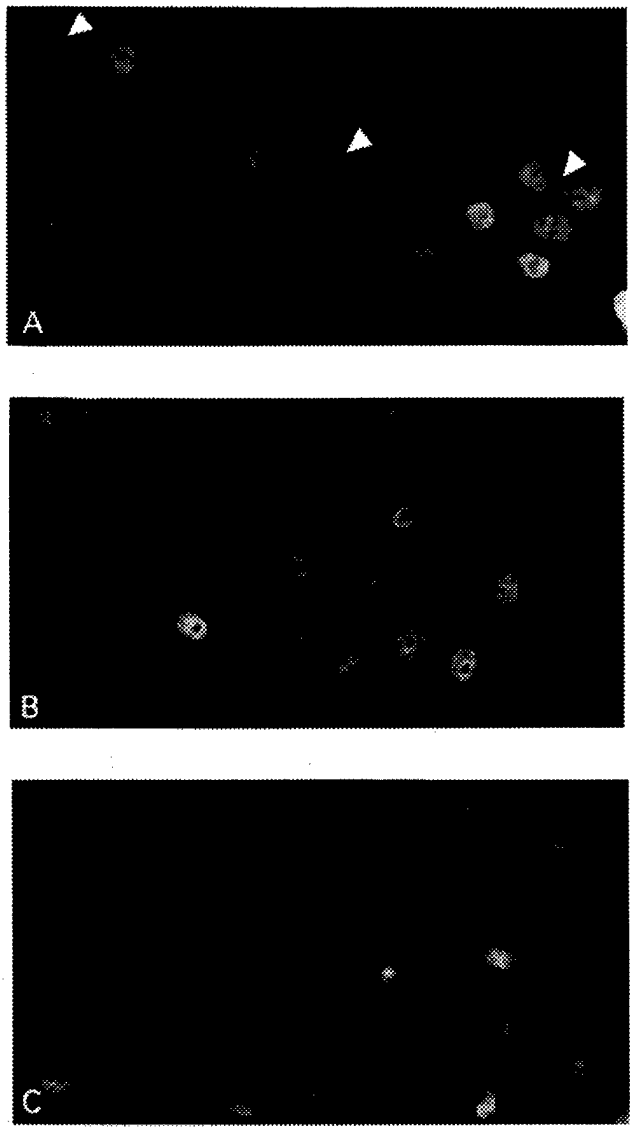

Figure 3. Overexpression of p21$^{WAF1/CIP1}$ does not affect *bcl*-2 inhibition of radiation-induced apoptosis. Nuclear morphologies of irradiated MCF10A (A), py3 (B) and p21-pp (C) cells were examined using bisBenzimide. Arrows indicate fragmented nucleus of apoptotic cells.

following irradiation. To this end, we introduced an SV-40 promoter driven p21$^{WAF1/CIP1}$ expression vector together with hygromycin resistant vector (Py3) into *bcl*-2 overexpressing MCF10A cells. Transfectants were selected with hygromycin and individual clones were isolated. The level of p21$^{WAF1/CIP1}$ was determined using Western blot analysis (Fig. 1) and the clone #2 was used for the following studies. To rule out the possibility of clonal variation, a dozen individual clones were pooled together and also included in this study. Hereafter, control vector alone transfected *bcl*-2 overexpressing MCF10A cells are referred as py3, clone #2 which is the p21$^{WAF1/CIP1}$ transfected *bcl*-2 overexpressing MCF10A clone as p21-#2, and the mixture of 12 clones which are p21$^{WAF1/CIP1}$ transfected *bcl*-2 overexpressing MCF10A cells as p21-pp. Although both the basal level of the p21$^{WAF1/CIP1}$ protein from cells grown at confluence and radiation-induced expression of p21$^{WAF1/CIP1}$ were dramatically suppressed by *bcl*-2 (8), the p21$^{WAF1/CIP1}$ protein was detectable in the exponentially growing *bcl*-2 overexpressing cells (Fig. 1, lane 1). The level of p21$^{WAF1/CIP1}$ in p21-#2 or p21-pp was approximately 5 fold higher than that in py3. To determine whether p21$^{WAF1/CIP1}$ has anti-proliferative activity in *bcl*-2 overexpressing breast epithelial cells, the growth curves of py3, p21-#2 and p21-pp were determined. As shown in Fig. 2, p21$^{WAF1/CIP1}$ overexpression resulted in marked growth inhibition of *bcl*-2 overexpressing MCF10A cells.

If *bcl*-2 downregulation of p21$^{WAF1/CIP1}$ is necessary for inhibition of radiation-induced apoptosis, *bcl*-2 would fail to prevent apoptosis in the presence of high levels of p21$^{WAF1/CIP1}$. If this is the case, p21$^{WAF1/CIP1}$ transfected *bcl*-2 MCF10A cells would undergo apoptotic cell death following radiation as do control MCF10A cells. However, if *bcl*-2 down-regulation of p21$^{WAF1/CIP1}$ is not associated with *bcl*-2 inhibition of apoptosis, transfection of p21$^{WAF1/CIP1}$ would not alter the ability of *bcl*-2 to protect apoptotic cell death upon irradiation. As shown in Fig. 3A, the nuclei of the parental MCF10A cells undergo apoptotic cell death following radiation exposure. The nuclei of MCF10A cells were fragmented into brightly stained round compartments, which is consistent with nuclear morphological changes in apoptotic cells (11). No apoptotic cells were detected in Py3 and p21-pp following radiation exposure. These data showthat *bcl*-2 downregulation of p21$^{WAF1/CIP1}$ is not required for *bcl*-2 inhibition of apoptosis in breast epithelial cells. To further support the conclusion that *bcl*-2 inhibits radiation-induced apoptosis in the presence of a high level of p21$^{WAF1/CIP1}$ expression, we examined the apoptosis-specific cleavage of poly(ADP-ribose) polymerase (PARP), since this cleavage is believed an early event in apoptosis resulted from activation of interleukin 1-converting enzyme (ICE, caspase)/*ced*-3 family (15). As shown in Fig. 4, PARP was processed proteolytically in floating MCF10A cells undergoing radiation-induced cell death. PARP cleavage was inhibited in MCF10A cells stably expressing *bcl*-2 alone or together with p21$^{WAF1/CIP1}$.

Radiation-induced apoptosis is not dose dependent and causes a relatively small reduction in clonogenic survival. The dose dependent radiation-induced cell lethality appears to be induced by mitotic-linked death resulting from loss of genetic information (12). The tumor suppressor gene p53 is associated with increased radiosensitivity in clonogenic survival assay, although the underlying mechanism is not clear (13). Although it was shown that expression of p21$^{WAF1/CIP1}$ is highly induced upon irradiation in a p53 dependent manner (8,16), the effect of p21$^{WAF1/CIP1}$ induction on radiosensitivity has not been determined. To examine the effect of p21$^{WAF1/CIP1}$ on the radiosensitivity of breast epithelial cells, we determined the dose-survival curves for py3, p21 #2 and p21-pp after radiation exposure. The multitarget dose-survival curve parameters D_0 (the reciprocal of the slope) and n (the extrapolation number) were extracted from the data shown in Fig. 4. The values of D_0 an n for py3 were 2.4 Gy and 1.8 respectively. Survival curves for py3 and p21$^{WAF1/CIP1}$ transfected cells were essentially

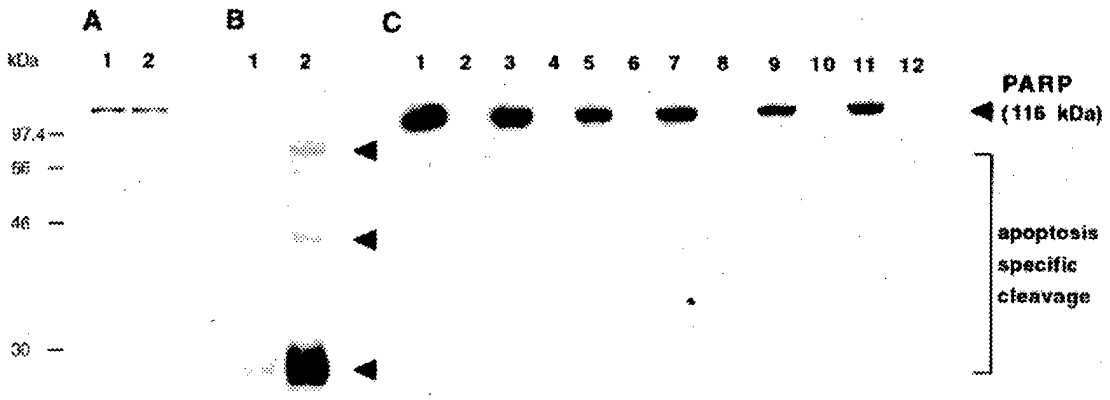

Figure 4. Apoptosis-specific cleavage of PARP in MCF10A cells undergoing radiation-induced cell death. Western blot analysis of PARP protein was performed to detect apoptosis-specific cleavage of PARP. The adherent cells and floating cells were collected separately at 24 h after irradiation at 6 Gy. A, Adherent MCF10A cells without irradiation (lane 1) and with irradiation (lane 2). B, Floating MCF10A cells without irradiation (lane 1) and with irradiation (lane 2). C, Adherent py3 cells without irradiation (lane 1) and with irradiation (lane 3), floating py3 cells without irradiation (lane 2) and with irradiation (lane 4), adherent p21-#2 cells without irradiation (lane 5) and with irradiation (lane 7), floating p21-#2 cells without irradiation (lane 6) and with irradiation (lane 8), adherent p21-pp cells without irradiation (lane 9) and with irradiation (lane 11), floating p21-pp cells without irradiation (lane 10) and with irradiation (lane 12).

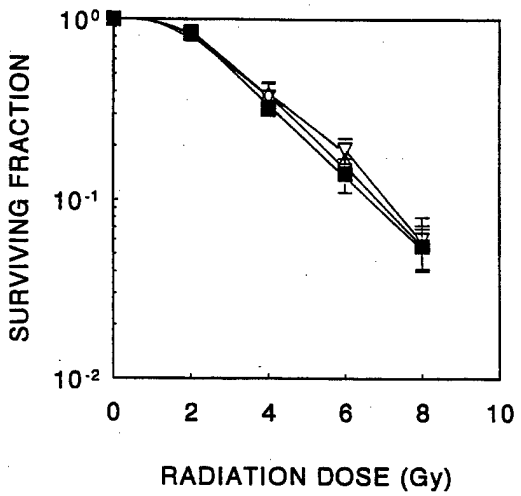

Figure 5. Cell survival curves following irradiation. Py3 (■), p21-#2 (Δ) and p21-pp (∇) cells were exposed to X-rays. Error bars represent standard deviation of the mean of three or four separate experiments.

superimposable for all radiation doses. These results show that p21$^{WAF1/CIP1}$ expression does not affect intrinsic radiosensitivity in these cells. This is consistent with the observation that p21$^{WAF1/CIP1}$ is dispensable for radiation induced apoptosis, although it is critical for p53-mediated cell cycle arrest (6,14,17,18). Our study, however, does not exclude the possibility of involvement of p21$^{WAF1/CIP1}$ in apoptosis induced by other stimuli. For example, when the E2F-1 encoding gene is introduced into cells that contain a temperature-sensitive p53 allele, coexpression of the wild-type p53 protein and transcription factor E2F induces apoptosis, suggesting that when the E2F-1 signal to enter the S phase confronts a p53-imposed delay of entry into S phase, p53 and E2F-1 together signal apoptosis (19). p21$^{WAF1/CIP1}$ may be critical for p53/E2F-1 induced apoptosis through its involvement in p53-mediated G_1 arrest. p21$^{WAF1/CIP1}$ may be a general regulator of apoptosis that is induced by G_1/S deregulation. Recently, involvement of p21$^{WAF1/CIP1}$ in apoptosis (20) or DNA repair (21) was also reported in retinoblastoma-negative human sarcoma cells (20). Whether or not p21$^{WAF1/CIP1}$ regulates other apoptosis pathways, our data clearly suggest that p21$^{WAF1/CIP1}$ is not involved in radiation-induced cell death in human breast epithelial cells.

Acknowledgments

This work was partially supported by NIH/NCI Grant (CA 64139), Institutional American Cancer Society Grant (IRG-162H) (to H-RC K), and NIH/NCI Grant (CA48000), WBHRI 96-03 (to YJL). H-RC K is a recipient of Career Development Award from the department of the Army. We thank Dr Stanley Korsmeyer for providing the *bcl*-2 expression vector and Bert Vogelstein for providing p21 WAF1/CIP1 cDNA probe. MCF10A cells were provided by the Karmanos Cancer Institute (NIH Core Grant CA22453).

References

1. Hollstein M, Sidransky D, Vogelstein B and Harris CC: p53 mutation in human cancers. Science 253: 49-53, 1991.
2. El-Deiry WS, Tokino T, Velculescu VE, Levy DB, Parsons R, Trent JM, Lin D, Mercer WE, Kinzler KW and Volgelstein B: WAF1, a potential mediator of p53 tumor suppression. Cell 75: 817-825, 1993.
3. Harper JW, Adami GR, Wei N, Keyomarsi K and Elledge JS: The p21 Cdk-interacting protein Cip1 is a potent inhibitor of G1 cyclin-dependent kinases. Cell 75: 805-816, 1993.
4. Xiong Y, Hannon GJ, Zhang H, Casso D, Kobayashi R and Beach D: p21 is a universal inhibitor of cyclin kinases. Nature 366: 701-704, 1993.
5. Noda A, Ning Y, Vanable SF, Pereira-Smith OM and Smith JR: Cloning of senescent cell derived inhibitors of DNA synthesis using an expression screen. Exp Cell Res 211: 90-98, 1994.

6. Waldman T, Kinzler KW and Vogelstein B: P21 is necessary for the p53-mediated G1 arrest in human cancer cells. Cancer Res 55: 5187-5190, 1995.
7. Chen YQ, Cipriano S, Arenkiel JM and Miller FR: Tumor suppression by $p21^{WAF1}$. Cancer Res 55: 4536-4539, 1995.
8. Upadhyay U, Li G, Liu H, Chen YQ, Sarkar FH and Kim HRC: *Bcl*-2 suppresses expression of $p21^{WAF1/CIP1}$ in breast epithelial cells. Cancer Res 55: 4520-4524, 1995.
9. Soule H, Maloney TM, Wolman SR, Petersom WD, Brenz R, McGrath CM, Russo J, Pauley RJ, Jones RF and Brooks SC: Isolation and characterization of a spontaneously immortalized human breast epithelial cell line, MCF-10. Cancer Res 50: 6075-6086, 1990.
10. Tait L, Soule HJ and Russo J: Ultrastructural and immunocytochemical characterization of an immortalized human breast epithelial cell line, MCF-10. Cancer Res 50: 6087-6094, 1990.
11. Deckwerth TL and Johnson EM: Temporal analysis of events associated with programmed cell death (apoptosis) of sympathetic neurons deprived of nerve growth factor. J Cell Biol 123: 1207-1222, 1993.
12. Dewey W, Ling C and Meyn R: Radiation-induced apoptosis: Relevance to radiotherapy. Int J Rad Oncol Biol Phys 33: 781-796, 1995.
13. Lowe SW, Ruley HE, Jacks T and Housman D: P53-dependent apoptosis modulates the cytotoxicity of anticancer agents. Cell 74: 957-967, 1993.
14. Deng C, Zhang P, Harper JW, Elledge SJ and Leder P: Mice lacking $p21^{CIP1/WAF1}$ undergo normal development, but are defective in G1 checkpoint control. Cell 82: 675-684, 1995.
15. Lazebnik YA, Kaufmann SH, Desnoyers S, Poirier GG and Earnshaw WC: Cleavage of poly (ADO-ribose) polymerase by a proteinase with properties like ICE. Nature 371: 346-347, 1994.
16. El-Deiry WS, Harper JW, O'Connor PM, Velculescu VE, Canman CE, Jackman J, Pietenpol JA, Burrell M, Hill DE, Wang Y, Wiman KG, Mercer WE, Kastan MB, Kohn KW, Elledge SJ, Kinzler KW and Vogelstein B: WAF1/Cip1 is induced in p53-mediated G1 arrest and apoptosis. Cancer Res 54: 1169-1174, 1994.
17. Deng C, Zhang P, Harper JW, Elledge SJ and Leder P: Mice lacking $p21^{CIP1/WAF1}$ undergo normal development, but are defective in G1 checkpoint control. Cell 82: 675-684, 1995.
18. Brugarolas J, Chandrasekaran C, Gordon JI, Beach D, Jacks T and Hannon GJ: Radiation induced cell cycle arrest compromised by p21 deficiency. Nature 377: 552-577, 1995.
19. Wu X and Levine AJ: P53 and E2F-1 cooperate to mediate apoptosis. Proc Natl Acad Sci USA 91: 3602-3606, 1994.
20. Li W, Fan J, Hochhauser D and Bertino JR: Overexpression of $p21^{waf1}$ leads to increased inhibition of E2F-1 phosphorylation and sensitivity to anticancer drug in retinoblastoma-negative human sarcoma cells. Cancer Res 57: 2193-2199, 1997.
21. McDonald III ER, Wu GS, Waldman T and El-Deiry WS: Repair defect in p21WAF1/CIP1 human cancer cells. Cancer Res 56: 2250-2255, 1996.

ELSEVIER

Int. J. Radiation Oncology Biol. Phys., Vol. 39, No. 2, pp. 000–000, 1997

0360-3016/97 $17.00 + .00

PII S0360-3016(97)00358-1

Biology

AQ1 ● ~~Clinical~~ *Original Contribution*

PLATELET-DERIVED GROWTH FACTOR (PDGF)-SIGNALING MEDIATES RADIATION-INDUCED APOPTOSIS IN HUMAN PROSTATE CANCER CELLS WITH LOSS OF P53 FUNCTION

HAROLD E. KIM, M.D.,* SUE J. HAN, M.D.,‡ THOMAS KASZA, M.S.,‡ RICHARD HAN, B.S.,† HYEONG-SEON CHOI, PH.D.,§ KENNETH C. PALMER, PH.D.† AND HYEONG-REH C. KIM, PH.D.*†‡

*Department of Radiation Oncology, †Department of Pathology, Wayne State University School of Medicine, Detroit, MI 48202, USA; ‡Department of Radiation Oncology, Veterans Administration Medical Center, Detroit, MI 48202; and §Department of Biology, Ewha Woman's University, Seoul, Korea

Platelet-derived growth factor (PDGF) signals a diversity of cellular responses *in vitro*, including cell proliferation, survival, transformation, and chemotaxis. PDGF functions as a "competence factor" to induce a set of early response genes expressed in G_1 including $p21^{WAF1/CIP1}$, a functional mediator of the tumor suppressor gene p53 in G_1/S checkpoint. For PDGF-stimulated cells to progress beyond G_1 and transit the cell cycle completely, progression factors in serum such as insulin and IGF-1 are required. We have recently shown a novel role of PDGF in inducing apoptosis in growth-arrested murine fibroblasts. The PDGF-induced apoptosis is rescued by insulin, suggesting that G_1/S checkpoint is a critical determinant for PDGF-induced apoptosis. Because recent studies suggest that radiation-induced signal transduction pathways interact with growth factor-mediated signaling pathways, we have investigated whether activation of the PDGF-signaling facilitates the radiation-induced apoptosis in the absence of functional p53. For this study we have used the 125-IL cell line, a mutant p53-containing, highly metastatic, and hormone-unresponsive human prostate carcinoma cell line. PDGF signaling is constitutively activated by transfection with a $p28^{v\text{-}sis}$ expression vector, which was previously shown to activate PDGF α- and β- receptors. Although the basal level of $p21^{WAF1/CIP1}$ expression and radiation-induced apoptosis were not detectable in control 125-IL cells as would be predicted in mutant p53-containing cells, activation of PDGF-signaling induced expression of $p21^{WAF1/CIP1}$ and radiation-induced apoptosis. Our study suggests that the level of "competence" growth factors including PDGF may be one of the critical determinants for radiation-induced apoptosis, especially in cells with loss of p53 function at the site of radiotherapy *in vivo*. © 1997 Elsevier Science Inc.

Platelet-derived growth factor, Radiation-induced apoptosis, Human prostate cancer cells.

INTRODUCTION

AQ3 Platelet-derived growth factor (PDGF) is composed of three dimeric polypeptide chains, the homodimers PDGF AA and BB, and the heterodimer PDGF AB. The A- and B-chains of PDGF are approximately 50% identical in amino acid sequence and have perfect conservation of cysteine residues (7, 16). The PDGF isoforms interact differentially with each of two (α and β) PDGF receptors. PDGF BB binds with high affinity to the PDGF α and β receptors, whereas PDGF AA interacts effectively only with the PDGF α receptor (5, 25). The B-chain is 92% homologous to the oncogene product ($p28^{v\text{-}sis}$) of the simian sarcoma virus, establishing a causative role of growth factors in malignancy. $p28^{v\text{-}sis}$/PDGF BB interacts with the PDGF receptors intracellularly and induces transformation (8, 9). In addition to proliferation and transformation, PDGF signals diverse cellular responses *in vitro*, including chemotaxis and cell survival that correlate with proposed functional roles of PDGF *in vivo* in normal development, inflammation, and wound healing and in the abnormal cell migration and proliferative responses characteristic of atherosclerosis, fibrosis, and neoplasia (7, 16).

PDGF functions in serum starved cells as a "competence" factor to stimulate expression of a set of immediate early-response genes including c-*myc*, c-*fos*, and actin during G_0/G_1 transition (12, 18, 21, 29). The mRNA levels of these genes are sharply reduced as cells transit through G_1/S. For PDGF to stimulate cells to progress beyond late G_1 and transit the cell cycle and divide, progression factors in serum such as insulin and IGF are required (29). We have recently shown a novel role for PDGF in inducing

Reprint requests to: Hyeong-Reh C. Kim, Ph.D., Department of [redacted]

Acknowledgments—This work was supported by grants from American Heart Association/MI (66GB956), NIH/NCI (CA 64139) (to H.-R.C.K). H.-R.C.K is a recipient of Career Development Award from the U.S. Army (DAMD17-96-1-6181). Authors thank Dr. Joy Ware for providing human prostatic carcinoma cell lines.

Accepted for publication 7 March 1997.

Pathology, Wayne State University School of Medicine, Detroit, MI 48201

apoptosis in growth arrested murine fibroblasts (19). Insulin rescues PDGF-induced apoptosis, suggesting that G_1/S checkpoint is an important determinant for PDGF-induced apoptosis (19).

Radiation induces not only postmitotic cell death but also other cellular responses including apoptosis, proliferation, inflammatory reaction, and fibrosis. Increasing evidence suggests that diverse responses of tumor cells following irradiation result from activation of different signal transduction pathways depending on genetic background of the cells [reviewed in (17)]. Irradiation of tissue containing H_2O generates reactive oxygen species or free radical that interact with cellular organelles including membrane and DNA. Radiation-induced signaling initiated from cytoplasmic membrane activates enzymes (e.g., PKC, raf-1 kinase) that are involved in growth factor-mediated signal transduction pathways, suggesting an interaction between radiation-signaling and growth factor-signaling [reviewed in (14)].

One of the most critical signaling molecules in radiation-induced cellular responses is the tumor suppressor gene product p53. Following irradiation, p53 induces apoptosis or regulates a G_1 checkpoint that arrests the cell cycle prior to the initiation of DNA synthesis. p53 induces transcription of its effector genes such as GADD45 and $p21^{WAF1/CIP1}$. $p21^{WAF1/CIP1}$, an inhibitor of cyclin-dependent kinases, is a functional mediator of p53-dependent cell cycle regulation at G_1/S checkpoint following irradiation (10, 13, 15, 32). While DNA damage-induced expression of $p21^{WAF1/CIP1}$ depends on the wild-type p53 function, $p21^{WAF1/CIP1}$ can be induced in a p53-independent manner by serum or purified growth factors, including PDGF, EGF (epidermal growth factor), and FGF (fibroblast growth factor), but not insulin (26).

Unlike radiation-induced cell cycle regulation at G_1/S, radiation-induced apoptosis is still not understood, although the wild-type activity of p53 appears to be critical. Recent studies, however, show that p53-independent apoptotic pathways exist following irradiation (22, 28). In this study, we investigated whether PDGF signaling is involved in activation apoptotic cell death following irradiation in 125-IL cells. 125-IL is a highly metastatic subclone of the human prostate carcinoma cell line PC-3 (30). PC-3 cells carry a nucleotide deletion at the codon 138 in the p53 gene and 125-IL has an additional mutation at the codon 223 (4). Growth of PC-3 and 125-IL cells are androgen independent *in vitro* and in animal (30). Because it is clinically important to understand apoptotic cell death in mutant p53-containing, hormone-independent, and highly metastatic prostate carcinoma cells, 125-IL cells were chosen for this study. To activate PDGF signaling in these cells, we ~~transfected~~ an $p28^{v\text{-}sis}$, which was previously well characterized to induce PDGF signaling by intracellular activation of the PDGF receptors (2, 20). We now report that activation of PDGF signaling induces apoptotic cell death following irradiation. This study suggests that growth factors *in vivo* may regulate cell fate positively or negatively at the sites of chemo- and/or radiotherapy.

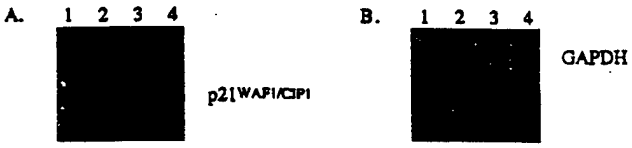

Fig. 1. 125-IL cells lost the wild-type p53 activity. (A) 125-IL cells were collected at 0 (lane 1) and 6 h (lane 2) after irradiation at a dose of 2 Gy using a 6 MeV electron beam. MCF7 cells were also collected at 0 (lane 3) and 6 h (lane 4) after irradiation. Cells are lysed in SDS gel electrophoresis buffer. The proteins were fractionated on a 16% SDS-polyacrylamide gel, electrophoretically blotted to nitrocellulose, and probed with anti-$p21^{WAF1/CIP1}$ antibody. (B) To control the amount of proteins loaded in each lane, the identical blot was probed with antiglyceraldehyde 3-phosphate dehydrogenase (GAPDH) antibody (Biologicals, MA).

METHODS AND MATERIALS

Transfection

The v-sis gene under the control of the Moloney murine leukemia virus long terminal repeats (2) was introduced into 125-IL cells (generously provided by Dr. J. Ware at the Medical College of Virginia) using Lipofectin (Sigma); 5×10^5 cells were plated on 100-mm dishes as previously described (20). The next day cells were washed with serum-free medium and overlaid with 5 ml of DMEM containing 10 μg of the v-sis expression vector DNA and 20 μl of Lipofectin. After 6 h, media was replaced with RPMI 1640 containing 5% fetal bovine serum. Stable transfectants were selected in the presence of 250 μg/ml G418 (geneticin sulfate).

Western blot analysis

To prepare whole cell extracts, cells were lysed using SDS sample buffer at a volume of 1×10^6 cells/100 μl.

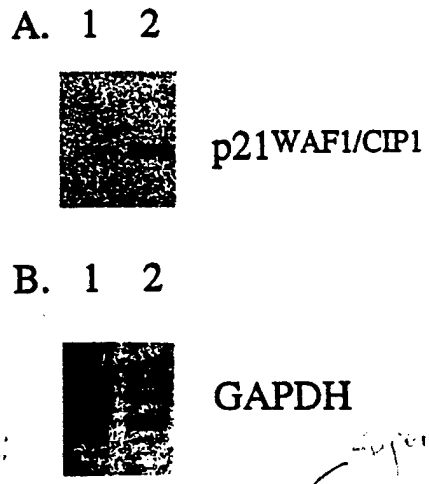

Fig. 2. Activation of PDGF-signaling pathway induces $p21^{WAF1/CIP1}$ in 125-IL cells. Control (lane 1) and p28v-sis expressing 125-IL cells (lane 2) were cultured in serum free medium for 2 days before protein extraction. Western blot analysis was performed as described in Fig. 1. (A) Levels of $p21^{WAF1/CIP1}$ was detected with anti-$p21^{WAF1/CIP1}$ antibody. (B) To control the amount of proteins loaded in each lane, the identical blot was probed with antiglyceraldehyde 3-phosphate dehydrogenase (GAPDH) antibody (Biologicals, MA).

4

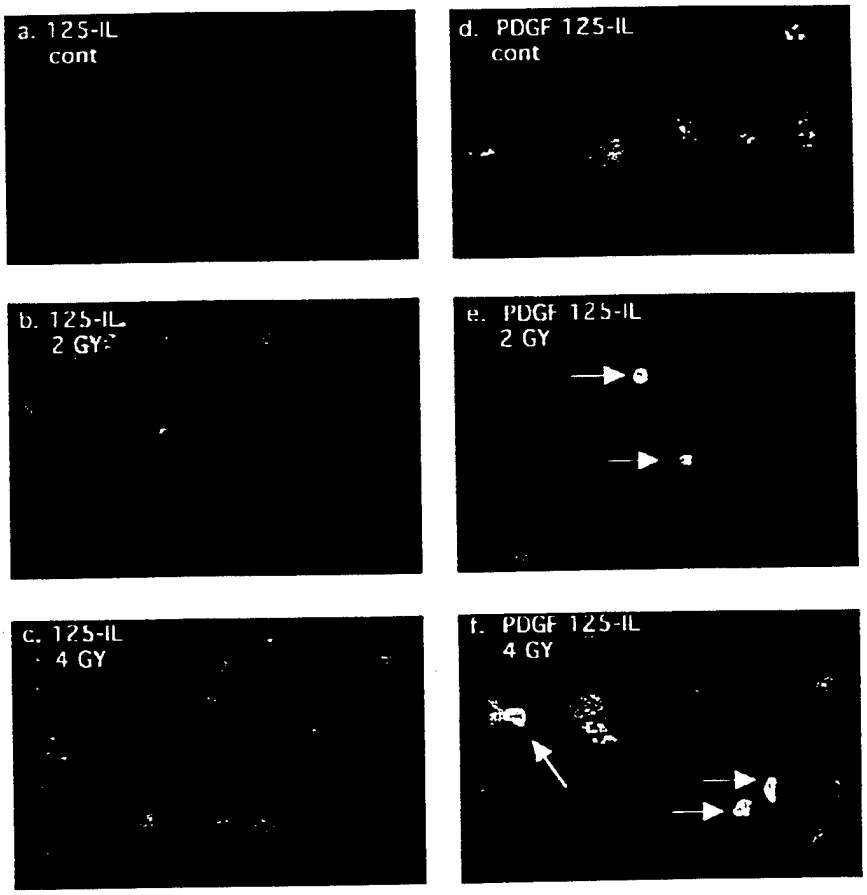

Fig. 3. Activation of PDGF-signaling pathway induces apoptosis in 125-IL cells. Control (a–c) and p28$^{v\text{-}sis}$-expressing (d–f) 125-IL cells were plated on a coverslip using RPMI medium containing 5% fetal calf serum. Next day, medium was replaced with serum-free RPMI medium. Two days later, cells were irradiated at 2 Gy (b and e) and 4 Gy (c and f). At 21 h of irradiation, cells were fixed and nuclei were stained with Bisbenzimide (Hoechst 33258).

Protein concentration was measured using BCA protein Assay Reagents (Pierce, IL). Cell extracts were boiled for 10 min and chilled on ice, subjected to 16% SDS-PAGE analysis, and then electrophoretically transferred to nitrocellulose membrane. The p21$^{WAF1/CIP1}$ protein was detected using anti-p21$^{WAF1/CIP1}$ antibody (Ab-1 from Oncogene Science).

Nuclear staining

125-IL and v-sis expressing 125-IL cells were plated on coverslips in a six-well plate. The next day cells were washed with PBS and incubated with serum-free medium for 2 days. Cells were then irradiated at 2 Gy and 4 Gy using a 6 MeV electron beam. One day postirradiation, cells were washed with PBS and fixed with 4% paraformaldehyde in PBS for at least 12 h. The coverslips were removed from the plate and cells were exposed to 1 μg/ml 2′-(4-hydroxyphenyl)-5-(4-methyl-1-piperazinyl)-2,5′-bi-1*H*-benzimidazole trihydrochloride pentahydrate (Bisbenzimide, Hoechst 33258; Molecular Probes, Eugene, OR) in PBS for 15 min at room temperature, and washed with PBS. The cells were mounted in 0.1% *p*-phenylene diamine and 90% glycerol in PBS. Nuclear morphology was examined under UV illumination on a fluorescent microscope.

Electron microscopy

Control and v-sis–expressing 125-IL cells were irradiated at 6 Gy. The following day, cells were scraped from cultures and washed three times with Hanks balanced salt solution (HBSS). The corresponding cell pellets were resuspended in 10 vol of fresh 1.0% glutaraldehyde–1.25% paraformaldehyde in 0.1 M sodium cacodylate buffer (pH 7.4) and allowed to fix overnight at 4°C. Cells were washed in cacodylate buffer, postfixed with 2% aqueous osmium tetroxide for 1 h, dehydrated through a graded ethanol series, and embedded in epoxy. Ultrathin sections were cut, contrasted with uranyl acetate and lead citrate, viewed, and photographed with a Philips EM 400.

RESULTS

To investigate the effects of activation of PDGF-signaling on radiation-induced apoptosis in mutant p53-containing tumors, we chose a prostate cancer cell line (125-IL),

which contains mutations in the p53 gene (4). To confirm that 125-IL cells do not have a wild-type function of p53, the induction of p53-dependent gene expression upon irradiation was examined (11). As shown in Fig. 1, $p21^{WAF1/CIP1}$ gene expression was not induced following irradiation in 125-IL cells, whereas it was highly induced in MCF7 cells that possess the wild-type p53 gene (1). This result shows that 125-IL cells lost the wild-type p53 activity, as would be expected from sequencing analysis of p53 gene in these cells (4). The basal level of $p21^{WAF1/CIP1}$ in 125-IL cells was significantly lower than the level in MCF7 cells (Fig. 1, lanes 1 and 3), a finding that is consistent with the published observation that the basal expression of $p21^{WAF1/CIP1}$ is dependent on the wild-type p53 function (11).

PDGF signaling was constitutively activated in 125-IL cells by transfection with $p28^{v\text{-}sis}$ expression vector. $p28^{v\text{-}sis}$ expression vector was chosen because it was previously well studied that the $p28^{v\text{-}sis}$ gene product interacts with PDGF receptors and activates signal transduction pathways (2, 20). After selection for cells with stably integrated plasmids, more than 200 clones were pooled together. Because it was previously reported that PDGF induces expression of $p21^{WAF1/CIP1}$ independent of p53 (26), we examined the levels of $p21^{WAF1/CIP1}$ expression in these transfected cells to assure activation of PDGF signaling. To exclude effects of growth factors (including PDGF) in serum, control and $p28^{v\text{-}sis}$-expressing 125-IL cells were cultured in serum-free medium for 2 days prior to protein extraction. As shown in Fig. 2, the basal level of $p21^{WAF1/CIP1}$ was significantly induced by intracellular expression of $p28^{v\text{-}sis}$ in those cells. This result shows that overexpression of ligand constitutively activated PDGF signaling in 125-IL cells.

We then explored the possibility that activation of PDGF signaling facilitates radiation-induced apoptosis in these cells. Because morphological assessment of dying cells is believed to be the most reliable method to detect apoptosis (24), the nuclear morphological changes of control and $p28^{v\text{-}sis}$-expressing 125-IL cells were analyzed following irradiation. As shown in Fig. 3, radiation did not induce nuclear morphological changes characteristic of apoptosis in control 125-IL cells as expected from cells with loss of the wild-type p53 activity. In contrast, the nuclei of $p28^{v\text{-}sis}$-expressing 125-IL cells were condensed and/or fragmented into brightly stained round compartments following irradiation. Table 1 shows an apoptotic index established by examining nuclear morphological changes of control and PDGF signaling-activated 125-IL cells. Whereas apoptotic cell death was barely detected in control cells upon irradiation, 5–8% of PDGF signaling-activated 125-IL cells committed to apoptotic cell death following irradiation. It was noted that approximately 1–2% of PDGF signaling-activated 125-IL cells underwent spontaneous apoptotic cell death when grown in serum-free medium for 3 days, and that radiation-induced apoptosis in PDGF signaling-activated 125-IL cells does not appear to be dose dependent.

Table 1. Effects of activation of PDGF signaling pathway on radiation-induced apoptosis in 125-IL cells

Cell	Radiation	No. of apoptotic cells/ total cells counted	% Apoptosis
125-IL	no	0/80, 0/76, 0/88	0%
	2 Gy	0/90, 0/81, 0/72	0%
	4 Gy	1/34, 0/100, 0/50	<1%
$p28^{v\text{-}sis}$-125-IL	no	1/100, 1/50, 1/68	1–2%
	2 Gy	3/45, 3/48, 5/100	5–7%
	4 Gy	2/40, 3/40, 6/100	5–8%

Apoptotic cells were identified by morphological analysis after 21 h of irradiation (as shown in Fig. 3).

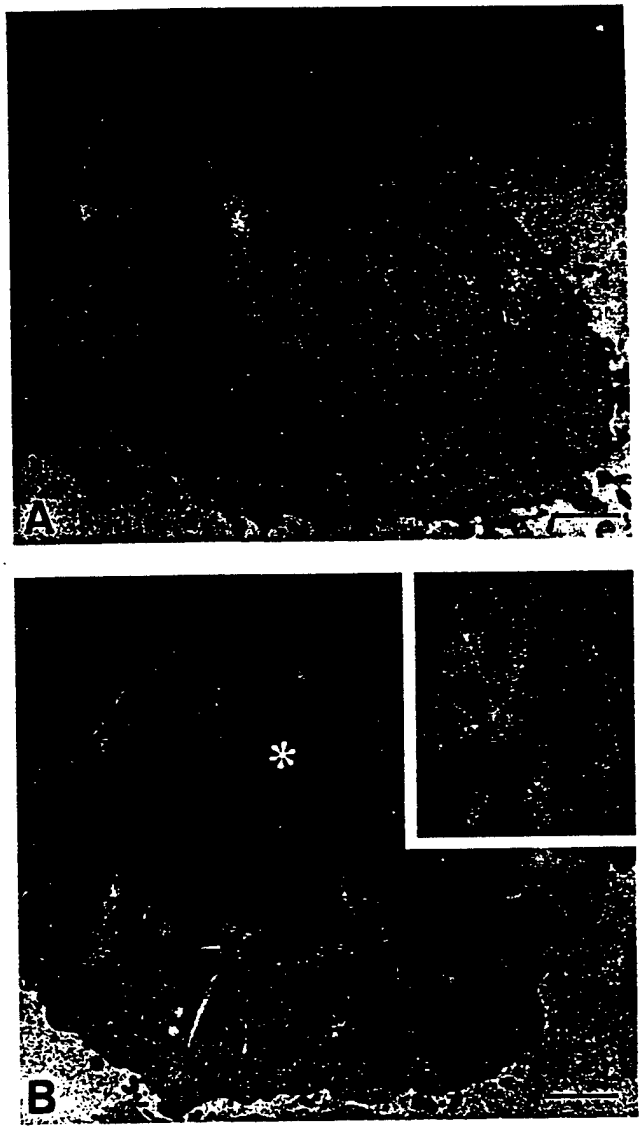

Fig. 4. Electron micrograph of an apoptotic cell. An electron micrograph of a control 125-IL cell (A) and PDGF-signaling activated 125-IL cell (B) following irradiation. The inset shows fragmented and condensed chromatin (asterisk) at higher magnification where a well-defined nuclear envelope can be seen (arrow).

Apoptotic cell death was also confirmed by electron microscopic analysis (Fig. 4). The ultrastructural appear-

ance of a control 125-IL cell is shown in Fig. 4A. This cell displayed normal morphology, with no evidence of ~~necrosis or~~ apoptotic alterations 24 h after irradiation at 6 Gy. Some expansion of the endoplasmic reticulum was visible, but this was minimal. An apoptotic cell of PDGF signaling-activated 125 IL cells following irradiation, shown in Fig. 4B, displayed markedly different morphological features. The cell was shrunken and condensed, and demonstrated condensation of chromatin into multiple dense masses. At high magnification (inset) an intact nuclear membrane surrounding these nuclear fragments (arrow) was visible. Blebbing of the plasma membrane, without rupture, and the presence of intact, membrane-limited lysosomal structures were characteristic of apoptotic cells. The present study show that activation of PDGF signaling interacts with radiation-induced signaling pathway, resulting in apoptotic cell death in mutant p53 containing human prostate cancer cells. These results suggest the potential of growth factor overexpression in cancer cells to regulate cell proliferation and fate at the site of radiotherapy.

DISCUSSION

In addition to the roles of PDGF in proliferation and transformation, PDGF appears to regulate cell fate when cells are within unfavorable environments for cell growth (19). In this study, we examined the effects of activation of PDGF signaling on radiation-induced cellular responses when cell growth is limited by culture in serum-free medium imposing a high degree of cell cycle arrest. The condition for cell cycle arrest was chosen instead of the conventional condition for cell survival assay using logarithmically growing cells, because tumor cell environment *in vivo* undergoing chemotherapy or radiation therapy may limit the potential of cells to completely transit the cell cycle.

There is mounting evidence that regulation of apoptosis plays an important role in tumor cell response to cytotoxic treatments. The genetic defects in the apoptotic pathway of tumor cells inversely correlate with relapse-free and overall survival after treatment (27). p53 status has been shown to correlate with the efficacy of cancer therapy *in vivo* (23). Following irradiation, p53 induces gene expression for G_1 arrest, DNA repair activity, and apoptosis (10, 11, 13, 15, 32). Recently, however, it was demonstrated that radiation-induced apoptosis can occur independent of p53 (22, 28). Our studies suggest that levels of "competence" growth factors such as PDGF may be one of the critical determinants for radiation-induced apoptosis independent of p53. Although many apoptotic stimuli have been identified *in vitro*, the biochemical pathways of apoptosis are poorly defined. This report suggests experimental strategies to investigate interactions of growth factor-induced signal transduction pathway and radiation-induced signal transduction pathway leading to p53-independent apoptosis. Because loss of wild-type activity of the tumor-suppressor gene p53 is one of the most frequent genetic defects in human cancer, understanding the p53-independent apoptotic pathway will be useful to develop new therapeutic strategies to treat mutant p53-containing tumors.

It is not clear whether $p21^{WAF1/CIP1}$ plays a role in PDGF-induced apoptosis following irradiation. As suggested in PDGF-induced apoptosis of serum-starved murine fibroblasts (19), G_1/S checkpoint may be critical in PDGF-induced apoptosis following irradiation. In this case, $p21^{WAF1/CIP1}$ may be involved in the regulation of G_1/S checkpoint leading to apoptosis. It is equally possible that PDGF induces apoptosis following irradiation independent of $p21^{WAF1/CIP1}$ and cell cycle regulation, as p53 mediates radiation-induced apoptosis independent of $p21^{WAF1/CIP1}$. $p21^{WAF1/CIP1}$ is dispensable for p53-dependent apoptosis, whereas it plays a critical role in p53-mediated G_1 arrest, as demonstrated in $p21^{WAF1/CIP1}$-deficient cell lines (3, 6, 31). Although we do not understand the mechanisms at the present time, our results suggest important insights into a potential new role of PDGF in the regulation of tumor cell growth and death *in vivo* in response to radiation therapy.

REFERENCES

1. Bartek, J.; Iggo, R.; Gannon, J.; Lane, D. P. Genetic and immunochemical analysis of mutant p53 in human breast cancer cell lines. Oncogene 5:893–899; 1990.
2. Bejeck, B.; Li, D.; Deuel, T. F. Transformation by v-sis occurs by an internal autoactivation mechanism. Science 245:1496–1499; 1989.
3. Brugarolas, J.; Chandrasekaran, C.; Gordon, J. I.; Beach, D.; Jacks, T.; Gregory, J. Hannon. Radiation-induced cell cycle arrest compromised by p21 deficiency. Nature 377:552–577; 1995.
4. Chen, Y. Q.; Gao, X.; Grignon, D.; Sarkar, F. H.; Sark, W.; Cipriano, S.; Honn, K. V.; Borders, J. S.; Crissman, J. D. Multiple mechanisms of p53 inactivation in prostatic carcinomas. Cell. Mol. Biol. 1:330–337; 1994.
5. Claesson-Welsh, L.; Eriksson, A.; Westermark, B.; Heldin, C.-H. cDNA cloning and expression of the human A-type platelet-derived growth factor (PDGF) receptor establishe structural similarity to the B-type PDGF receptor. Proc. Natl. Acad. Sci. USA 86:4917–4921; 1989.
6. Deng, C.; Zhang, P.; Harper, J. W.; Elledge, S. J.; Leder, P. Mice lacking $p21^{CIP1/WAF1}$ undergo normal development, but are defective in G_1 checkpoint control. Cell 82:675–684; 1995.
7. Deuel, T. F. Polypeptide growth factors: Roles in normal and abnormal cell growth. Annu. Rev. Cell Biol. 3:443–492; 1987.
8. Deuel, T. F.; Huang, J. S.; Huang, S. S.; Stroobant, P.; Waterfield, M. D. Expression of a platelet-derived growth factor-like protein in simian sarcoma virus transformed cells. Science 221:1348–1350; 1983.
9. Doolittle, R. F.; Hunkapiller, M. W.; Hood, L. E.; Devare, S. G.; Robbins, K. C.; Aaronson, S. A.; Antoniades, X. Simian sarcoma virus onc gene, v-sis, is derived from the gene (or genes) encoding a platelet-derived growth factor. Science 221: 275–277; 1983.

10. El-Deiry, W. S.; Tokino, T.; Velculescu, V. E.; Levy, D. B.; Parsons, R.; Trent, J. M.; Lin, D.; Mercer, W. E.; Kinzler, K. W.; Vogelstein, B. WAF1, a potential mediator of p53 tumor suppression. Cell 75:817–825; 1993.
11. El-Deiry, W. S.; Harper, J. W.; O'Connor, P. M.; Velculescu, V. E.; Canman, C. E.; Jackman, J.; Pietenpol, J. A.; Burrell, M.; Hill, D. E.; Wang, Y. WAF1/CIP1 is induced in p53-mediated G1 arrest and apoptosis. Cancer Res. 54:1169–1174; 1994.
12. Greenberg, M. E.; Ziff, E. B. Stimulation of 3T3 cells induces transcription of the c-fos proto-oncogene. Nature 311:433–438; 1984.
13. Gujuluva, C. N.; Baek, J.-H.; Shin, K.-H.; Cherrick, H. M.; Park, N.-H. Effect of UV-irradiation on cell cycle, viability, and the expression of p53, gadd 153, and gadd 45 genes in normal and HPV-immortalized human oral keratinocytes. Oncogene 9:1819–1827; 1994.
14. Hallahan, D. E. Radiation-mediated gene expression in the pathogenesis of the clinical radiation response. Semin. Radiat. Oncol. 6:250–267; 1996.
15. Harper, J. W.; Adami, G. R.; Wei, N.; Keyomarsi, K.; Elledge, S. J. The p21 Cdk-interacting protein Cip1 is a potent inhibitor of G1 cyclin-dependent kinases. Cell 75:805–816; 1993.
16. Heldin, C.-H. Structural and functional studies on platelet-derived growth factor. EMBO J. 11:4251–4259; 1992.
17. Jung, M. And Dritschilo Signal transduction and cellular responses to ionizing radiation. Semin. Radiat. Oncol. 6:268–283; 1996.
18. Kelly, K.; Cochran, B. H.; Stiles, C. D.; Leder, P. Cell-specific regulation of the c-myc gene by lymphocyte mitogens and platelet-derived growth factor. Cell 35:603–610; 1983.
19. Kim, H.-R. C.; Upadhyay, S.; Li, G.; Palmer, K. C.; Deuel, T. F. Platelet-derived growth factor (PDGF) induces apoptosis in growth arrested murine fibroblasts. Proc. Natl. Acad. Sci. USA 92:9500–9504; 1995.
20. Kim, H.-R. C.; Upadhyay, S.; Korsemeyer, S.; Deuel, T. F. Platelet-derived growth factor (PDGF) B and A homodimers transform murine fibroblasts depending on the genetic background of the cell. J. Biol. Chem. 269:30604–30608; 1994.
21. Lau, L. F.; Nathan, D. Identification of a set of gene expressed during the G0/G1 transition of cultured mouse cells. EMBO J. 4:3145–3151; 1985.
22. Lowe, S. W. Cancer therapy and p53. Curr. Opin. Oncol. 7:547–753; 1995.
23. Lowe, S. W.; Bodis, S.; McClatchey, A.; Remington, L.; Ruley, H. E.; Fisher, D.; Housman, D. E.; Jacks, T. p53 status and the efficacy of cancer therapy in vivo. Science 266:807–810; 1994.
24. Martin, J. S.; Green, D. R.; Cotter, T. G. Dicing with death: Dissecting the components of the apoptosis machinery. Trends Biochem. Sci. 19:26–30; 1994.
25. Matsui, T.; Heidaran, M.; Miki, T.; Popescu, N.; LaRochelle, W.; Kraus, M.; Pierce, J.; Aaronson, S. Isolation of a novel receptor cDNA establishes the existence of two PDGF receptor genes. Science 243:800–804; 1989.
26. Michieli, P.; Chedid, M.; Lin, D.; Pierce, J. H.; Mercer, W. E.; Givol, D. Induction of WAF1/CIP1 by a p53-independent pathway. Cancer Res. 54:3391–3395; 1994. → Daidone
27. Silvestrinii, R.; Veneroni, X.; Daidone, M. G.; Benini, E.; Boracchi, P.; Mezzetti, M.; Di Fronzo, G.; Rilke, F.; Veronesi, U. The bcl-2 protein: A prognostic indicator strongly related to p53 protein in lymph node-negative breast cancer patients. J. Natl. Cancer Inst. 86:499–504; 1994. AQ2 AQ4
28. Strasser, A.; Harris, A. W.; Jacks, T.; Cory, S. DNA damage can induce apoptosis in proliferating lymphoid cells via p53-independent mechanisms inhibitable by bcl-2. Cell 79:329–339; 1994.
29. Stiles, C. D.; Capone, G. T.; Scher, C. D.; Antoniades, H. N.; Van Wyk, J. J.; Pledger, W. J. Dual control of cell growth by somatomedins and platelet-derived growth factor. Proc. Natl. Acad. Sci. USA 76:1279–1283; 1979.
30. Ware, J. L. Prostate tumor progression and metastasis. Biochem. Biophys. Acta 907:279–298; 1987.
31. Waldman, T.; Kinzler, K. W.; Vogelstein, B. p21 is necessary for the p53-mediated G1 arrest in human cancer cells. Cancer Res. 55:5187–5190; 1995.
32. Xiong, Y.; Hannon, G. J.; Zhang, H.; Casso, D.; Kobayashi, R.; Beach, D. p21 is a universal inhibitor of cyclin kinases. Nature 366:701–704; 1993.

Author Queries

AQ1	Au: Please provide section title if different from one provided.
AQ2	Au: Please supply author's initial.
AQ3	Au: All references were renumbered to conform to journal style - please check all changes carefully.
AQ4	Au: Something missing?
AQ1	Biology Original Contribution
AQ2	Ref. 9 Antoniades, H. N.
	Ref. 27 Veneroni, S.; Daidone, M. G.; Benini E.;
AQ4	the title is O.K. (nothing is missing)
AQ3	Ref. look OK
	Additional Changes : 8